arXiv:1604.05556v2 [cond-mat.dis-nn] 26 Jul 2016

Universal correlations between shocks in the ground state of elastic interfaces in disordered media

Thimothée Thiery, Pierre Le Doussal and Kay Jörg Wiese
CNRS-Laboratoire de Physique Théorique de l'Ecole Normale Supérieure, PSL Research University, Sorbonne Universités, UPMC, 24 rue Lhomond,75005 Paris, France.

The ground state of an elastic interface in a disordered medium undergoes collective jumps upon variation of external parameters. These mesoscopic jumps are called shocks, or static avalanches. Submitting the interface to a parabolic potential centered at w, we study the avalanches which occur as w is varied. We are interested in the correlations between the avalanche sizes S_1 and S_2 occurring at positions w_1 and w_2. Using the Functional Renormalization Group (FRG), we show that correlations exist for realistic interface models below their upper critical dimension. Notably, the connected moment $\langle S_1 S_2 \rangle^c$ is up to a prefactor *exactly* the renormalized disorder correlator, itself a function of $|w_2 - w_1|$. The latter is the universal function at the center of the FRG; hence correlations between shocks are universal as well. All moments and the full joint probability distribution are computed to first non-trivial order in an ϵ-expansion below the upper critical dimension. To quantify the local nature of the coupling between avalanches, we calculate the correlations of their local jumps. We finally test our predictions against simulations of a particle in random-bond and random-force disorder, with surprisingly good agreement.

PACS numbers: 05.40.-a, 05.10.Cc, 64.60.av

I. INTRODUCTION

The model of an elastic interface in a disordered medium has been put forward as a relevant description for a large number of systems [1–4]. Examples include domain walls in soft magnets [5, 6], fluid contact lines on a rough surface [7, 8], strike-slip faults in geophysics [9, 10], fracture in brittle materials [11–13] or imbibition fronts [14]. An important common property of these systems is that their response to an applied field is not smooth but rather proceeds via jumps extending over a broad range of space and time scales. As a consequence, understanding the properties and the universality of avalanche processes has received a lot of attention in the past years [15–17].

A problem of outstanding interest is to quantify the correlations between successive avalanches. In the context of earthquakes those are linked to the notion of *aftershocks*, whose statistics is characterized through phenomenological laws such as the Omori law [18]. Several mechanisms have been advanced to explain these strong correlations, all involving an additional dynamical variable [19, 20]. For elastic interfaces, correlations between avalanches were yet only studied as a result of such additional degrees of freedom in the interface dynamics, as relaxation processes [21, 22] or memory effects [23]. In this work, we show that even in the absence of such mechanisms, *avalanches in elastic interfaces are generically correlated below their upper critical dimension.* These correlations are universal.

Let us emphasize that the goal of this paper is *not* to understand or explain the aftershock statistics observed in earthquakes, for which additional mechanisms such as those discussed above are necessary. Rather, it is to emphasize that for disordered elastic systems, *except for mean-field models, correlations between avalanches always exist.* A precise quantitative understanding of these correlations is necessary to correctly quantify correlations induced by additional mechanisms. In systems where the description by the standard elastic-interface model is accurate (without additional mechanisms) our results quantify the correlations between avalanches. To our knowledge, these correlations have up to now been ignored in theoretical or experimental work. It would thus be interesting to quantify them better, in order to access universality, or lack thereof, in various avalanche processes.

In this article we study the correlations between the sizes and locations of shocks in the ground state (also called "static avalanches") of elastic interfaces in disordered media. These static avalanches are close cousins of the (dynamic) avalanches observed in the interface dynamics at depinning. As we discuss below, we expect most of our results to hold for both classes. Our study is conducted using the Functional Renormalization Group (FRG). Originally introduced as a powerful tool to study the universal properties of the statics and dynamics (at the depinning transition) of elastic interfaces in disordered media [24–30], the FRG has been recently adapted to the study of avalanches [31–36]. It has notably led to a rigorous identification of the relevant mean-field theory for the statistics of single avalanches: the Brownian-Force Model (BFM), a multidimensional generalization of the celebrated Alessandro-Beatrice-Bertotti-Montorsi (ABBM) model [37, 38]. Interestingly, the FRG allows to go beyond mean-field theory and to compute in a controlled way avalanche observables in an expansion in $\epsilon = d_{\rm uc} - d$ where d is the interface dimension, and $d_{\rm uc}$ the upper critical dimension of the problem. The latter depends on the range of the elastic interactions, with $d_{\rm uc} = 4$ for short-ranged (SR) elasticity and $d_{\rm uc} = 2$ for the usual long-ranged (LR) elasticity.

The outline of this article is as follows: In section II we summarize our results, preceded by a definition of the relevant observables. In Section III we introduce the model and the observables we are interested in. Section IV contains the derivation of the main results presented above. Section V gives an analysis of the correlations between the local shock sizes. Section VI presents the results of our numerical analysis of these correlations for a toy model with a single degree of freedom, i.e. $d = 0$. Finally, a series of appendices contains technical derivations.

II. MAIN RESULTS

Let us now state our main results for interfaces with a short-ranged elastic kernel (a more general case will be treated in the manuscript, with little changes to the formulas). To this aim, we parameterize the position of the interface by the (real, one-component) displacement field $u(x)$, where $x \in \mathbb{R}^d$ is the internal coordinate of the interface. For notational convenience we denote $u(x) \equiv u_x$. The interface is submitted to a quenched random potential $V(u_x, x)$, and to an external parabolic confining field $\frac{m^2}{2}(u_x - w)^2$ centered at w. In a given disorder realization V, upon variation of the external fiel w, the ground state (i.e. lowest-energy) configuration of the interface, denoted $u_x(w)$, changes discontinuously at a set of discrete locations w_i, according to

$$u_x(w_i^-) \to u_x(w_i^+) = u_x(w_i^-) + S_x^{(i)} \ . \tag{1}$$

The event $(w_i, S_x^{(i)})$ is the i^{th} shock of the interface, w_i is the location of the shock, $S_x^{(i)}$ is its local size at x and $S^{(i)} = \int d^d x \, S_x^{(i)}$ its total size. The statistical properties associated to one shock were thoroughly analyzed using FRG in [31, 32]. Such properties are encoded in the *shock density* ρ_0, defined as

$$\rho_0 := \overline{\sum_i \delta(w - w_i)} \ , \tag{2}$$

and in the *avalanche-size density*

$$\rho(S) := \overline{\sum_i \delta(w - w_i)\delta(S - S^{(i)})} \ . \tag{3}$$

The *shock-size density* $\rho(S)$ is linked to ρ_0 through $\rho_0 = \int dS \, \rho(S)$. Note that these quantities do not depend on w due to the statistical translational invariance (STS) of the disorder. Considering two points $w < w'$ and sizes $S_1 < S_2$, $\int_w^{w'} d\tilde{w} \int_{S_1}^{S_2} dS \rho(S)$ is the mean number of shocks occurring between w and w' with size $S \in [S_1, S_2]$, while $(w' - w)\rho_0$ is the mean number of shocks (irrespective of their size). Note that throughout the rest of this section we will discuss our results in terms of densities but they can be translated into results for normalized probabilities as we discuss in Sec. III E.

These observables alone do not determine the statistical properties of the sequence $\{(w_i, S^{(i)})\}_{i\in\mathbb{Z}}$ of shocks experienced by the interface in a given environment. In particular, they do not contain any information about the correlations between the shocks. For a given distance $W > 0$, let us therefore introduce the *two-shock density at distance W*,

$$\rho_2(W) := \overline{\sum_{i\neq j} \delta(w - w_i)\delta(w + W - w_j)} \ . \tag{4}$$

This observable scales as *the square of a density*. Thus $\int_{w_1}^{w_1'} dw \int_{w_2}^{w_2'} dw' \rho_2(w' - w)$ counts *the mean number of pairs of shocks* such that the first shock occurs between w_1 and w_1', and the second one between w_2 and w_2'. Equivalently, $\tilde{\rho}_2(W) := \frac{\rho_2(W)}{\rho_0}$ is the density of shocks at a distance W from a given shock. These observables contain information about the correlations between shocks. Indeed an uncorrelated sequence of shocks implies $\rho_2(W) = \rho_0^2$ (and thus $\tilde{\rho}_2(W) = \rho_0$). A central question addressed in this work is whether the presence of a shock at a given point decreases ($\rho_2(W) < \rho_0^2$) or increases ($\rho_2(W) > \rho_0^2$) the density of shocks at a distance W.

To measure the correlations between the size of the shocks (and not only their positions) we introduce the *two-shock size density* at distance W,

$$\rho_W(S_1, S_2) := \overline{\sum_{i\neq j} \delta(w - w_i)\delta(S_1 - S^{(i)})\delta(w + W - w_j)\delta(S_2 - S^{(j)})} \ . \tag{5}$$

It is linked to $\rho_2(W)$ via

$$\rho_2(W) = \int dS_1 \, dS_2 \, \rho_W(S_1, S_2) \ . \tag{6}$$

Here $\int_{w_1}^{w_1'} dw \int_{w_2}^{w_2'} dw' \int_{S_1}^{S_1'} dS \int_{S_2}^{S_2'} dS' \rho_{w'-w}(S, S')$ counts the mean number of pairs of shocks such that the first shock occurred between w_1 and w_1', and the second between w_2 and w_2', with sizes between S_1 and S_1', resp. S_2 and S_2'. For this observable, an absence of correlations in the sequence of shocks implies $\rho_W(S_1, S_2) = \rho(S_1)\rho(S_2)$. To investigate the presence of correlations we thus study the *connected two-shock size density* $\rho_W^c(S_1, S_2)$, defined as

$$\rho_W^c(S_1, S_2) := \rho_W(S_1, S_2) - \rho(S_1)\rho(S_2) \ . \tag{7}$$

At the level of mean-field theory, i.e. in the BFM model, it is known [32, 35] that the shocks are independent and the process $w \to u_x(w)$ is a Levy jump process. As a consequence, $\rho_W^c(S_1, S_2) = 0$. On the other hand, for realistic interface models below their upper critical dimension, the shocks are correlated, demanding to go beyond the BFM. This can be seen from the second moment for which we show below the *exact* relation

$$\frac{\langle S_1 S_2 \rangle_{\rho_W^c}}{[\langle S \rangle_\rho]^2} = -\frac{\Delta''(W)}{L^d m^4} \ . \tag{8}$$

On the left-hand-side, $\langle ... \rangle_{\rho^c_W}$ denotes the average with respect to ρ^c_W as defined in Eq. (7). On the right-hand-side, L is the lateral extension of the system, and m^2 the curvature of the confining potential, which sets the correlation length $L_m := 1/m$ for avalanches in the lateral direction. Finally, $\Delta(W)$ is the renormalized disorder-force correlator, the central object in the FRG treatment of disordered elastic systems: Denoting $u(w)$ the center-of-mass position of the interface, given well-position w, the correlator $\Delta(W)$ is defined as the connected correlation function of the center-of-mass fluctuations of the interface position [39],

$$\Delta(W) := L^d m^4 \overline{[u(w) - w]\,[u(w+W) - (w+W)]}^c \ . \tag{9}$$

Up to a universal scaling factor and a single non-universal scale, the function $\Delta(W)$ only depends on the universality class of the problem. It was computed up to two-loop accuracy in Ref. [30] and measured numerically in Ref. [40]. For our purpose it is important that the function $\Delta(W)$ is uniformly of order ϵ, and that its second derivative is non-zero. Thus the correlations (8) increase when going away from the upper critical dimension, where mean-field theory, or equivalently the BFM is relevant. Indeed, for the BFM $\Delta''(W) = 0$, and the effective disorder force is distributed as a Brownian motion. Beyond mean-field theory, the sequence of shocks is correlated, thus the effective disorder force at large scales has a different statistics than Brownian motion. The sign of these correlations depends on the sign of $\Delta''(W)$, which, in turn, depends on the universality class of the problem. As detailed in Sec. III C, *our results predict qualitatively different correlations depending on the universality class.* The most important static universality classes of non-periodic, short-ranged disorder are the random-bond (RB) universality class, which at the microscopic level has short-ranged potential-potential correlations, and the random-field (RF) universality class, for which the force-force correlations, but not the potential-potential correlations, are short-ranged at the microscopic level. As is summarized in Fig. 1, for RF-disorder $\Delta''(W) > 0$, and thus avalanches are always anti-correlated. On the other hand, for RB-disorder, avalanches are anti-correlated at short distances W, but positively correlated at larger ones.

To obtain results for higher avalanche-size moments, we use the FRG and the $\epsilon = (d_{\rm uc} - d)$ expansion to show that, to lowest non-trivial order in the expansion,

$$\rho^c_W(S_1, S_2) = -\frac{\Delta''(W)}{L^d m^4} \frac{S_1 S_2}{4 S_m^2} \rho(S_1)\rho(S_2) + O(\epsilon^2) \ . \tag{10}$$

Here

$$S_m := \frac{\langle S^2 \rangle_\rho}{2 \langle S \rangle_\rho} \ , \tag{11}$$

where $\langle ... \rangle_\rho$ denotes the average with respect to ρ as defined in Eq. (3), is the characteristic size of avalanches,

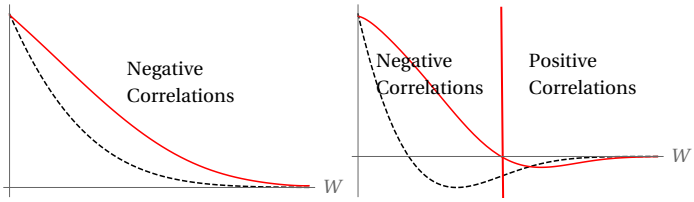

FIG. 1: Cartoons of the typical shape of the renormalized disorder correlator $\Delta(W)$ (black-dashed line) and of its second order derivative $\Delta''(W)$ (red line) for the Random-Field (left) and Random-Bond (right) universality classes (not to scale). Our results predict that the shock sizes are always negatively correlated in the Random-Field universality class, whereas the Random-Bond universality class exhibits a richer structure with negatively (resp. positively) correlated shock sizes at small (resp. large) distances.

which acts as a large-scale cutoff for the avalanche-size density $\rho(S)$, and $\Delta''(W)$ introduced above is $O(\epsilon)$. Integrating Eq. (10) times $S_1 S_2$ over S_1 and S_2, we recover Eq. (8). Contrary to the latter equation which is exact, relation (10) is correct only to order ϵ.

As a consequence of Eq. (10), and its generalizations to higher order, the correlations between avalanches are universal. To make this more transparent, we rewrite Eq. (10) as

$$\rho^c_W(S_1, S_2) = \frac{1}{(Lm)^d} \frac{L^{2d}}{S_m^4} \mathcal{F}_d\Big(\frac{W}{W_m}, \frac{S_1}{S_m}, \frac{S_2}{S_m}\Big) \ . \tag{12}$$

The function $\mathcal{F}_d$ is universal and apart from its three arguments depends only on the spatial dimension. To first order in $d = d_{\rm uc} - \epsilon$, and in the limit of large L and small m, it is given by

$$\mathcal{F}(w, s_1, s_2) \simeq \frac{A_d \tilde{\Delta}^{*\prime\prime}(w)}{16\pi\sqrt{s_1 s_2}} e^{-(s_1+s_2)/4} + O(\epsilon^2) \ . \tag{13}$$

Here A_d is an explicit constant, with $A_{d=4} = 8\pi^2$ for SR elasticity; the scale $W_m \sim m^{-\zeta}$, with ζ the roughness exponent contains a non-universal amplitude. The range of validity of this result is discussed in the main text. The presence of the factor of $1/(Lm)^d$ highlights the fact that the correlations between shocks are local (indeed $N := (Lm)^d$ counts the number of elastically independent regions of the interface). We will analyze this local structure by studying the correlations between the local sizes of the shocks.

To summarize, let us emphasize again our main message namely that for realistic models (beyond mean-field) the sequence of shocks is always correlated.

III. MODEL, SHOCK OBSERVABLES AND METHOD

A. Model

Consider the Hamiltonian for a $d-$dimensional elastic interface with position $u(x) \equiv u_x \in \mathbb{R}$ ($x \in \mathbb{R}^d$), elastic kernel $g^{-1}_{xx'}$, subjected to a harmonic well centered at w, and to a disorder potential $V(u,x)$:

$$\mathcal{H}[u;w] = \frac{1}{2}\int_{xx'} g^{-1}_{xx'}(u_x - w)(u_{x'} - w) + \int_x V(u_x, x) \ . \tag{14}$$

Here $\int_x = \int d^d x$ and we assume everywhere that the system is confined in a box of length L with e.g. periodic boundary conditions (the boundary conditions will not play a role in the following). We also assume the existence of a short-scale length cutoff a. The elastic kernel is translationally invariant ($g^{-1}_{xx'} = g^{-1}_{x-x'}$) and defines a convex elastic-energy functional (i.e. $g^{-1}_{xx'} > 0$ for $x \neq x'$). We denote $g^{-1}_q = 1/g_q$ its Fourier transform defined as $g^{-1}_q = \int_q e^{iqx} g^{-1}_x$, where $\int_q = \int \frac{d^d q}{(2\pi)^d}$. A possible choice is the standard short-ranged elasticity defined by

$$g^{-1}_{xx'} = \delta_{xx'}(-\nabla^2_{x'} + m^2) \quad , \quad g^{-1}_q = q^2 + m^2 \ . \tag{15}$$

Here $\delta_{xx'}$ is the Dirac δ distribution, and the elastic coefficient has been set to one using an appropriate choice of units. Another kernel we consider is

$$g^{-1}_q = (q^2 + \mu^2)^{\frac{\gamma}{2}} \ , \tag{16}$$

where $\gamma = 2$ corresponds to the previous case, and $\gamma = 1$ is relevant for long-ranged elasticity, as encountered in fracture and contact-line experiments. For a kernel of the form (16) we define the mass term as

$$m^2 := g^{-1}_{q=0} = \mu^\gamma. \tag{17}$$

It is the strength of the harmonic well. For short-ranged elasticity we have

$$\begin{aligned} \mathcal{H}_{\rm el}[u;w] &:= \frac{1}{2}\int_{xx'} g^{-1}_{xx'}(u_x - w)(u'_x - w) \\ &= \frac{1}{2}\int_x (\nabla_x u_x)^2 + m^2(u_x - w)^2. \end{aligned} \tag{18}$$

Thus $L_m := m^{-1}$ defines a length scale beyond which different parts of the interface are elastically independent. It also provides a large-scale cutoff in loop integrals encountered in the field theory. For more general kernels (16) this length scale is $L_\mu := \mu^{-1}$, and we suppose $L_\mu \ll L$, ensuring that boundary conditions do not play a role. The number of elastically independent parts of the interface is $N = (L/L_\mu)^d$. The disordered potential $V(u,x)$ is assumed to be short-ranged in internal space x, and statistically translationally invariant, with a second cumulant

$$\overline{V(u,x)V(u',x')}^c = \delta_{xx'} R_0(u - u') \ . \tag{19}$$

The overline $\overline{(...)}$ denotes the average over the disorder, and superscript c stands for connected averages. The detailed form of R_0 is, apart from global features that determine the universality class of the problem (see Sec. III C), unimportant. We also consider the force-force cumulant $\Delta_0(u) = -R_0''(u)$ such that $\overline{\partial_u V(u,x)\partial_{u'} V(u',x')}^c = \delta_{xx'}\Delta_0(u-u')$. Introducing a (finite) temperature T, disorder and thermal averages in this model can efficiently be computed using a replicated field theory. Introducing n replicated fields u_{ax}, $a = 1, \dots, n$, the replicated action reads

$$\begin{aligned} S[u] \ &= \ \frac{1}{2T}\sum_a \int_{xx'} g^{-1}_{xx'}(u_{ax} - w)(u_{ax'} - w) \\ &\quad - \frac{1}{2T^2}\sum_{a,b}\int_x R_0(u_{ax} - u_{bx}) + \cdots \end{aligned} \tag{20}$$

where $\cdots$ indicates eventual higher cumulants of the disorder.

B. The ground state and the scaling limit

As discussed in the introduction, we are interested in the minimal energy configuration of the interface for a given parabolic well position w and disorder realization V(i.e. the $T = 0$ problem). It is defined as the configuration $u_x(w)$, which minimises the energy,

$$u_x(w) := \underset{u_x}{\rm argmin}\ \mathcal{H}[u;w] \ . \tag{21}$$

We denote

$$u(w) := \frac{1}{L^d}\int_x u_x(w), \tag{22}$$

the center of mass of the ground-state of the interface. The statistical properties of $u_x(w)$ have been extensively studied in the literature. In particular it is known that the interface is self-affine with a (static) roughness exponent ζ, defined by $\overline{[u_x(w) - u_{x'}(w)]^2} \sim |x - x'|^{2\zeta}$. This scaling form generally holds in the scaling regime $L_c \ll |x - x'| \ll L_\mu$ where L_c is the Larkin length. The scaling limit is thus obtained for $L_\mu \to \infty$ or equivalently for $\mu \to 0$, also equivalent to $m \to 0$ (see (17)), a regime which is implicit throughout this work. In the FRG treatment of this problem, the ground state statistics is studied using the replicated field theory (20). The mass term m (or $\mu = m^{2/\gamma}$) can be conveniently used as a control parameter to study the flow of the effective action. As $m \to 0$ and through a proper rescaling, the effective action approaches a RG fixed point. This fixed point is perturbative in $\epsilon = d_{\rm uc} - d > 0$ where $d_{\rm uc}$ is the upper critical dimension of the model (for kernels of the form (16) it is given by $d_{\rm uc} = 2\gamma$, thus $d_{\rm uc} = 4$ for short-ranged elasticity and $d_{\rm uc} = 2$ for long-ranged elasticity). The central object of the theory is the effective disorder correlator $R(u)$, a renormalized version of $R_0(u)$. It appears in the effective action of the theory $\Gamma[u]$, as $R_0(u)$

appears in the bare action $S[u]$ of Eq. (20) (see the action (57) below). Remarkably, as shown in Ref. [41], it is related to a physical observable, the renormalized disorder force-force correlator $\Delta(u)$ defined as

$$\Delta(w-w') := L^d m^4 \overline{[u(w)-w][u(w')-w']}^c \ , \qquad (23)$$

through the relation $\Delta''(u) = -R(u)$. This is the function that appears in the results (8) and (10) of the introduction. The RG flow can be equivalently studied on R or Δ. For $m \to \infty$, the correlator $\Delta(w)$ is equal to the bare force-force correlator: $\Delta(w) \to_{m\to\infty} \Delta_0(w)$. In the limit $m \to 0$ it admits a scaling form

$$\Delta(w) = A_d \mu^{\epsilon-2\zeta} \tilde{\Delta}(\mu^\zeta w) \qquad (24)$$

where A_d is a dimensionless constant, and we recall $\mu = m^{2/\gamma}$. For kernels of the form (16), a convenient choice is to take A_d as $A_d = \frac{1}{\epsilon \tilde{I}_2}$ with the dimensionless loop integral $\tilde{I}_2 := \int_q \frac{1}{(1+q^2)^\gamma}$. Note that the combination $\epsilon \tilde{I}_2$ stays finite as $\epsilon \to 0$. In general

$$A_d^{-1} = \epsilon \tilde{I}_2 = \frac{2}{(2\sqrt{\pi})^d} \frac{\Gamma(\gamma+1-d/2)}{\Gamma(\gamma)} \ , \qquad (25)$$

and for example $\epsilon \tilde{I}_2 =_{\gamma=2;d=4} 1/(8\pi^2)$ and $\epsilon \tilde{I}_2 =_{\gamma=1;d=2} 1/(2\pi)$. As $m \to 0$, the rescaled disorder correlator $\tilde{\Delta}$ converges to the fixed point of the FRG flow equation $\tilde{\Delta}^*(u)$, which depends only on the universality class.

Let us now recall some important properties of these fixed-point functions.

C. Properties of $\tilde{\Delta}^*(u)$ and static universality classes

Depending on the properties of the bare disorder correlator $R_0(u)$, the FRG predicts that $\tilde{\Delta}(u)$ converges as $m \to 0$ to one of the fixed point of the FRG equation. A property of the (zero-temperature) FRG equation is that, for non-periodic disorder, if $\tilde{\Delta}^*(u)$ is a fixed point, $\kappa^2 \tilde{\Delta}^*(u/\kappa)$ also is a fixed point. Hence the fixed point towards which the system flows contains one non-universal scale whose value depends on microscopic properties of the disorder. The known fixed points can be regrouped into four main classes[1]. Analytic properties of these fixed-point functions are known up to two-loop order, i.e. $O(\epsilon^2)$, see Ref. [30] to which we refer the reader for quantitative results. An important property is that all fixed points exhibit a cusp around 0, $\Delta(u) \simeq \Delta(0) + \Delta'(0^+)|u| + O(u^2)$, related to the presence of avalanches [31, 33]. For our analys the sign of $(\Delta^*)''(u)$ is crucial as it determines the sign of the correlations. From the exact result (8) (shown below) we see that for $(\tilde{\Delta}^*)''(W) > 0$ shock sizes at distance W are anti-correlated, whereas for $(\tilde{\Delta}^*)''(W) < 0$) they are positively correlated.

Random-bond: This class has a bare disorder potential $V(x,u)$ distributed with short-ranged correlations in the u direction: The bare disorder correlator $R_0(u)$ decays quickly to 0 as $u \to \infty$. The most important property for our analysis of the fixed-point function $\tilde{\Delta}^*_{\rm RB}(u)$ (its typical form is plotted on the right of Fig. 1) is that $(\tilde{\Delta}^*_{\rm RB})''(u) > 0$ at small u and $(\tilde{\Delta}^*_{\rm RB})''(u) < 0$ at large u.

Random field: This class has the bare disorder force $F(x,u) = -\partial_u V(x,u)$ distributed with short-ranged correlations. Then the bare force-force correlator $\Delta_0(u)$ is short-ranged and $R_0(u) \simeq_{u\gg 1} -\sigma|u|$ where σ is called the amplitude of the random field. The most important property for our analysis of the fixed point function $\tilde{\Delta}^*_{\rm RF}(u)$ (its typical form is plotted on the left of Fig. 1) is that $(\tilde{\Delta}^*_{\rm RF})''(u) > 0$ for all x.

Random periodic: This class corresponds to periodic disorder $V(u+1) = V(u)$. As a consequence, $\tilde{\Delta}^*(u)$ is also periodic and $(\tilde{\Delta}^*)''(u) = (\tilde{\Delta}^*)''(0) > 0$ is constant. Though our analysis still applies to this universality class and our results are correct to $O(\epsilon)$, we will not discuss it here. As the shock process is periodic in any dimension, correlations naturally arise from this periodicity (in particular in $d = 0$ in the $m \to 0$ limit only one shock survives per interval).

The Brownian-Force-Model universality class: Finally, the Brownian-Force-Model defined as $\Delta_0(u) = -\sigma|u|$ is also a fixed point of the FRG flow equation and attracts all bare disorder such that $\Delta_0(u) \simeq -\sigma'|u|$ at large u. It models avalanches at the mean-field level. (It resums tree diagrams). In this model shocks are uncorrelated.

Hence, from the perspective of practical applications, the *qualitative* behavior of the correlations between shocks as a function of the distance strongly depends on the universality class of the model (see Fig. 1).

D. Shocks observables: Densities

As recalled in the introduction, it is well known that in the limit of small m the (rescaled) ground state $u_x(w)$ is piecewise constant as a function of w. In terms of the sequence of shocks $\{(w_i, S_x^{(i)})\}_{i\in\mathbb{Z}}$ one can write $u_x(w)$ and $u(w)$ as

$$\begin{aligned} u_x(w) &= \sum_i \theta(w-w_i) S_x^{(i)} \ , \\ u(w) &= \frac{1}{L^d} \sum_i \theta(w-w_i) S^{(i)} \ , \end{aligned} \qquad (26)$$

[1] There are other classes with different long-range correlations, but we will not study them.

where $\theta(x)$ is the Heaviside theta function. We recall the definition of the one and two-shock size-density:

$$\rho(S) = \overline{\sum_i \delta(w - w_i)\delta(S - S^{(i)})} \ , \tag{27}$$

$$\rho_W(S_1, S_2) = \overline{\sum_{i\neq j} \delta(w - w_i)\delta(S_1 - S^{(i)})\delta(w + W - w_j)\delta(S_2 - S^{(j)}))} \ . \tag{28}$$

These distributions possess a large-scale cutoff which we denote S_m; the latter diverges for m to 0 as $S_m \sim m^{-d-\zeta}$. Additionally, we suppose that they have a small-scale cutoff S_0. In the scaling regime, $\rho(S)$ behaves as a power law with a characteristic exponent τ: $\rho(S) \sim S^{-\tau}$ for $S_0 \ll S \ll S_m$. We us also define the connected density

$$\rho^c_W(S_1, S_2) = \rho_W(S_1, S_2) - \rho(S_1)\rho(S_2) \ . \tag{29}$$

In the first part of this work our goal is to compute $\rho^c_W(S_1, S_2)$ up to first order in ϵ using the FRG.

E. Shocks observables: Probabilities

One can normalize the above densities to define proper probability distributions as follows:

$$\rho_0 \ := \ \int \rho(S)\, dS \ , \tag{30}$$

$$\rho_2(W) \ := \ \int \rho_W(S_1, S_2)\, dS_1\, dS_2 \ , \tag{31}$$

$$P(S) \ := \ \frac{\rho(S)}{\rho_0} \ , \tag{32}$$

$$P_W(S_1, S_2) \ := \ \frac{\rho_W(S_1, S_2)}{\rho_2(W)} \ . \tag{33}$$

With this definition, $\rho_0 dw$ is the mean number of avalanches occurring in an interval dw and $\int_{w_1}^{w_2} dw \int_{w_3}^{w_4} dw' \rho_2(w' - w)$ counts the number of pairs of shocks where the first one occurs between w_1 and w_2 and the second between w_3 and w_4, irrespective of their sizes. Given these definitions, $P(S)$ and $P_W(S)$ are normalized probability distribution functions (PDF). $\int_S^{S'} d\tilde{S}\, P(\tilde{S})$ is the probability, given that a shock has occurred, that its size is between S and S'. $\int_{S_1}^{S_1'} dS \int_{S_2}^{S_2'} dS' P_W(S, S')$ is the probability, given that two shocks occurred at a distance W, that their sizes are between S_1 and S_1', and S_2 and S_2'. Note that a priori the marginal distribution $\int dS_1 P_W(S_1, S_2)$ is different from $P(S_2)$ since it contains the additional information that a shock occurred at a distance W. At the level of these PDFs, the absence of correlations would imply $P_W(S_1, S_2) = P(S_1, S_2)$ and, though in the remaining of the text we will favor the use of densities, our results can be translated to probabilities using Eq. (33). As discussed in Ref. [31], for an avalanche-size distribution $\rho(S)$ with exponent $\tau > 1$ (which is relevant here), the value of ρ_0 is dominated by the small-scale cutoff S_0 for avalanche sizes, and diverges as $S_0 \to 0$,

$$\rho_0 = \int_{S_0}^{\infty} \rho(S) dS \sim_{S_0 \to 0} S_0^{1-\tau} \ . \tag{34}$$

Hence, ρ_0 is non-universal. In the same way $\rho_2(W)$ is non-universal, even though its relation with ρ_0 has some universal features as we will show below. We denote by $\langle ... \rangle_\rho$, $\langle ... \rangle_{\rho_W}$, $\langle ... \rangle_{\rho^c_W}$, $\langle ... \rangle_P$ and $\langle ... \rangle_{P_W}$ the averages with respect to ρ, ρ_W, ρ^c_W, P and P_W.

F. Relation between avalanche-size moments and renormalized force cumulants: First moment

The n^{th} cumulant of the renormalized pinning force is defined as

$$m^{2n}\overline{[u(w_1) - w_1] \dots [u(w_n) - w_n]}^c = (-1)^n L^{-(n-1)d} \hat{C}^{(n)}(w_1, \dots, w_n) \ . \tag{35}$$

By definition $\hat{C}^{(2)}(w_1, w_2) = \Delta(w_1 - w_2)$ as introduced above. By parity invariance of the disorder $m^2\overline{[u(w) - w]} = 0$, and thus $\hat{C}^{(1)}(w) = 0$.

First cumulant: One immediately gets by inserting Eq. (26) into $m^2\overline{[u(w) - w]} = 0$ the exact relation

$$\langle S \rangle_\rho = \rho_0 \langle S \rangle_P = L^d \ . \tag{36}$$

Second cumulant: Differentiating with respect to w_1 and w_2 the definition $L^{-d}\Delta(w_1 - w_2) = m^4\overline{[u(w_1) - w_1][u(w_2) - w_2]}$ with Eq. (26) inserted, one obtains the relation (33) of [31] (with a corrected misprint $1 \to -1$). It can be written in the form

$$-\frac{\Delta''(w_1 - w_2)}{L^d m^4} = L^{-2d}\langle S^2 \rangle_\rho \delta(w_1 - w_2) + L^{-2d}\langle S_1 S_2 \rangle_{\rho_{w_2 - w_1}} - 1 \ . \tag{37}$$

Hence, as pointed out in Ref. [31], the singular part of the second derivative of $\Delta''(w_1 - w_2)$ around $w_2 = w_1$ gives an exact relation between the cusp in the renormalized disorder correlator

$$\sigma := -\Delta'(0^+) = R'''(0^+) \ , \tag{38}$$

and the second avalanche-size moment,

$$S_m := \frac{\langle S^2 \rangle_\rho}{2\langle S \rangle_\rho} = \frac{\langle S^2 \rangle_P}{2\langle S \rangle_P} = \frac{\sigma}{m^4}. \tag{39}$$

The avalanche size S_m plays the role of a large-scale cutoff for $\rho(S)$. On the other hand, the regular part of Eq. (37) gives the exact relation

$$L^{-2d}\langle S_1 S_2 \rangle_{\rho_W} = 1 - \frac{\Delta''(W)}{L^d m^4}. \tag{40}$$

For uncorrelated shocks we would have obtained $L^{-2d}\langle S_1 S_2\rangle_{\rho_W} = 1$. The correlations thus come from the non-zero value of $\Delta''(W) \neq 0$, a property which is generally expected from the FRG. It is a simple signature of the fact that the effective disordered force felt by the interface at large scale is not Brownian. Note that in terms of the moments of the connected density, the exact relation (40) reads

$$L^{-2d}\langle S_1 S_2\rangle_{\rho_W^c} = -\frac{\Delta''(W)}{L^d m^4}. \tag{41}$$

Let us also write the exact relation (40) in terms of the probabilities defined in Sec. III E:

$$\frac{\rho_2(W)}{\rho_0^2}\frac{\langle S_1 S_2\rangle_{P_W}}{(\langle S\rangle_P)^2} = 1 - \frac{\Delta''(W)}{L^d m^4}. \tag{42}$$

G. Generating functions

We now introduce the generating functions which encode all the moments of the density $\rho_W(S_1, S_2)$. Let us first recall the generating functions used in the one-shock case:

$$\begin{aligned} Z(\lambda) &= L^{-d}\langle e^{\lambda S} - 1\rangle_\rho \ , \\ \hat{Z}(\lambda) &= L^{-d}\langle e^{\lambda S} - \lambda S - 1\rangle_\rho = Z(\lambda) - \lambda. \end{aligned} \tag{43}$$

They are related to observables associated with the position as

$$\begin{aligned} Z(\lambda) &= L^{-d}\lim_{\delta\to 0^+}\partial_\delta \overline{e^{L^d[u(w+\delta)-u(w)]}} \ , \\ \hat{Z}(\lambda) &= L^{-d}\lim_{\delta\to 0^+}\partial_\delta \overline{e^{L^d[\hat{u}(w+\delta)-\hat{u}(w)]}} \ , \end{aligned} \tag{44}$$

where $\hat{u}(w) := u(w) - w$ is the translated position field. Note that due to STS they are independent of w. These relations were proven in Ref. [32]. For two shocks we introduce

$$Z_W(\lambda_1, \lambda_2) := L^{-2d}\langle (e^{\lambda_1 S_1} - 1)(e^{\lambda_2 S_2} - 1)\rangle_{\rho_W} \ . \tag{45}$$

We show in Appendix A that it can be computed as

$$\begin{aligned} &Z_W(\lambda_1, \lambda_2) \\ &= \hat{Z}_W(\lambda_1, \lambda_2) + \lambda_2\hat{Z}(\lambda_1) + \lambda_1\hat{Z}(\lambda_2) + \lambda_1\lambda_2 \\ &= \hat{Z}_W(\lambda_1, \lambda_2) + \lambda_2 Z(\lambda_1) + \lambda_1 Z(\lambda_2) - \lambda_1\lambda_2 \ . \end{aligned} \tag{46}$$

We used the definition

$$\hat{Z}_{w_2-w_1}(\lambda_1, \lambda_2) := L^{-2d} \times \lim_{\delta_1,\delta_2\to 0^+}\partial_{\delta_1,\delta_2}\overline{e^{L^d\lambda_1[\hat{u}(w_1+\delta_1)-\hat{u}(w_1)]}e^{L^d\lambda_2[\hat{u}(w_2+\delta_2)-\hat{u}(w_2)]}} \tag{47}$$

In the following we compute $\hat{Z}_W(\lambda_1, \lambda_2)$ using the FRG through formula (47). Let us also define the connected generating functions

$$\begin{aligned} Z_W^c(\lambda_1, \lambda_2) &:= L^{-2d}\langle (e^{\lambda_1 S_1} - 1)(e^{\lambda_2 S_2} - 1)\rangle_{\rho_W^c} \\ &= Z_W(\lambda_1, \lambda_2) - Z(\lambda_1)Z(\lambda_2) \\ \hat{Z}_W^c(\lambda_1, \lambda_2) &:= \hat{Z}_W(\lambda_1, \lambda_2) - \hat{Z}(\lambda_1)\hat{Z}(\lambda_2) \end{aligned} \tag{48}$$

These functions are actually equal: $Z_W^c(\lambda_1, \lambda_2) = \hat{Z}_W^c(\lambda_1, \lambda_2)$ as is easily seen using (46).

H. Relation between avalanche-size moments and renormalized force cumulants: Kolmogorov cumulants and chain rule

Using Eq. (47) and the fact that $\overline{\hat{u}(w)} = 0$, the generating function $\hat{Z}_W(\lambda_1, \lambda_2)$ can be written as

$$\hat{Z}_W(\lambda_1, \lambda_2) = \sum_{n,m=1}^{\infty}\frac{\lambda_1^n\lambda_2^m}{n!m!}\lim_{\delta_1,\delta_2\to 0^+} \frac{L^{(n+m-2)d}}{\delta_1\delta_2}\overline{[\hat{u}(\delta_1) - \hat{u}(0)]^n[\hat{u}(W+\delta_2) - \hat{u}(W)]^m} \ . \tag{49}$$

In the limit of $\delta_i \to 0$ we encounter for each (n, m) two types of terms:

$$\begin{aligned} &\overline{[\hat{u}(\delta_1) - \hat{u}(0)]^n[\hat{u}(W+\delta_2) - \hat{u}(W)]^m} = \\ &\quad \overline{[\hat{u}(\delta_1) - \hat{u}(0)]^n}^c \times \overline{[\hat{u}(W+\delta_2) - \hat{u}(W)]^m}^c \\ &\quad + \overline{[\hat{u}(\delta_1) - \hat{u}(0)]^n[\hat{u}(W+\delta_2) - \hat{u}(W)]^m}^c + O(\delta_i^3) \ . \end{aligned} \tag{50}$$

The term in the second line of Eq. (50) produces the disconnected part of the avalanche moment $\langle S_1^n\rangle\langle S_2^m\rangle$ and thus the disconnected part of the generating function $\hat{Z}_W(\lambda_1, \lambda_2)$, that is $\hat{Z}(\lambda_1)\hat{Z}(\lambda_2)$. The last term on the other hand contributes to $\langle S_1^n S_2^m\rangle_{\rho_W^c}$ and to the connected part of the generating function, $\hat{Z}_W^c(\lambda_1, \lambda_2) = Z_W^c(\lambda_1, \lambda_2)$ which is the true unknown. Introducing the Kolmogorov cumulants

$$K_W^{(n,m)}(\delta_1, \delta_2) := L^{(n+m-2)d}\overline{[\hat{u}(\delta_1) - \hat{u}(0)]^n[\hat{u}(W+\delta_2) - \hat{u}(0)]^m}^c \ , \tag{51}$$

we can write

$$Z_W^c(\lambda_1, \lambda_2) = \sum_{n,m=1}^{\infty}\frac{\lambda_1^n\lambda_2^m}{n!m!}\lim_{\delta_1,\delta_2\to 0^+}\frac{1}{\delta_1\delta_2}K_W^{(n,m)}(\delta_1, \delta_2) \ , \tag{52}$$

or, equivalently,

$$\langle S_1^n S_2^m\rangle_{\rho_W^c} = \lim_{\delta_1,\delta_2\to 0^+}\frac{1}{\delta_1\delta_2}K_W^{(n,m)}(\delta_1, \delta_2) \ . \tag{53}$$

The Kolmogorov cumulants (51) can be generally extracted from the renormalized force cumulants (35), as we now explain. Let us introduce[2]

$$C^{(n,m)}(w_1, \dots, w_n, w_{n+1}, \dots, w_{n+m}) = L^{(n+m-2)d}\overline{\hat{u}(w_1)\dots\hat{u}(w_n)\hat{u}(w_{n+1})\dots\hat{u}(w_{n+m})}^c \ . \tag{54}$$

[2] Note that those differ from $\mathcal{C}$ introduced in [31] by an additional factor of L^{-d}.

They are trivially linked to the renormalized force cumulants (35): $C^{(n,m)}(w_1,\dots,w_n,w_{n+1},\dots,w_{n+m}) = \frac{1}{L^d}(-1/m^2)^{n+m}\hat{C}^{(n+m)}(w_1,\dots w_{n+m})$. Explicit expressions for the lowest cumulants with $n+m \leq 4$ are displayed in Ref. [31], see e.g. Eq. (61) there. In the notation for $C^{(n,m)}$, though the expression is symmetric in w_i, we have highlighted the facts that in the end the n first w_i will be taken around $w=0$, whereas the last m will be around W. Indeed, to obtain $K_W^{(n,m)}(\delta_1,\delta_2)$ from the moments $C^{(n,m)}$, we must successively evaluate $C^{(n,m)}$ with $w_i \to \delta_1$ minus $C^{(n,m)}$ with $w_i \to 0$ for each $i=1,\dots,n$, then set $w_i \to W+\delta_2$ minus $C^{(n,m)}$ with $w_i \to W$ for each $i=n+1,\dots,n+m$. Ambiguities associated with the possible presence of terms such as $\Delta'(0^{\pm})$, are lifted by taking the limit of coinciding points with a given specific ordering of the w_i. Consistency requires that the end result does not depend on the chosen ordering, a property linked to the assumption that all singularities of the field $\hat{u}(w)$ can be modeled by a finite density of dilute shocks (which guarantees e.g. the continuity of $\hat{C}$). This iterative procedure was called the $\mathcal{K}$ operation in [31].

I. Strategy of the calculation and validity of the results

In order to compute $\hat{Z}_W(\lambda_1,\lambda_2)$, we must be able to perform disorder averages of moments of the position field at various positions w_i for $i=1,\dots,r$. For example $r=4$ is sufficient in the formulation (47) and used in Appendix D. In the main part of this work we report a calculation of $\hat{Z}_W(\lambda_1,\lambda_2)$ from the study of the moments (54) and we thus need to keep r arbitrary. We therefore consider the theory for r position fields u_x^i coupled to different parabolic wells centered at positions w_i in the same disordered environment. The Hamiltonian of the problem is

$$\mathcal{H}[\{u\},\{w\}] = \sum_{i=1}^{r} \mathcal{H}_{\rm el}[u^i,w^i] + \sum_{i=1}^{r}\int_x V(u_x^i,x) \ . \quad (55)$$

This leads to a replicated action of the form

$$\begin{aligned} S[u] &= \frac{1}{2T}\sum_{a,i}\int_{xx'} g^{-1}_{xx'}(u^i_{ax}-w_i)(u^i_{ax'}-w_i) \\ &\quad -\frac{1}{2T^2}\sum_{a,i;b,j}\int_x R_0(u^i_{ax}-u^j_{bx}) + \cdots \end{aligned} \quad (56)$$

The effective action of the theory is [31, 32, 41]

$$\begin{aligned} \Gamma[u] &= \frac{1}{2T}\sum_{a,i}\int_{xx'} g^{-1}_{xx'}(u^i_{ax}-w_i)(u^i_{ax'}-w_i) \\ &\quad -\frac{1}{2T^2}\sum_{a,i;b,j}\int_x R(u^i_{ax}-u^j_{bx}) + O(\epsilon^2) \ . \end{aligned} \quad (57)$$

Here $R(u) = O(\epsilon)$ is the renormalized disorder correlator already introduced in the previous section, while the neglected terms are higher-order terms in ϵ that can be expressed as loop integrals with higher powers of R. The calculation of observables using the effective action (57) has been called the *improved tree approximation* [31, 32]. Here we did not specify the number of replicas $a=1,\dots,n_r$. As is usual in replica calculations, the $n_r \to 0$ limit will be implicit in the following. Since (57) is the effective action, observables will be computed using a saddle-point calculation, or equivalently in a diagrammatic language, by resuming all tree diagrams generated by the action (57). This calculation allows to get the lowest order in ϵ for any observable. Let us recall the known results at the improved tree level for $\rho(S)$ and $Z(\lambda)$ as obtained in Refs. [31, 32]:

$$\rho(S) = \frac{L^d}{2\sqrt{\pi}S^{\frac{3}{2}}(S_m)^{\frac{1}{2}}} e^{-\frac{S}{4S_m}} \ , \quad (58)$$

$$Z(\lambda) = \lambda + S_m Z(\lambda)^2 = \frac{1}{2S_m}(1-\sqrt{1-4\lambda S_m}) \ . \quad (59)$$

J. Connected versus non-connected averages and the ϵ-expansion

Before going further, let us now mention a subtle point. As will become clear in the following, the improved tree calculation leads to a result of order $O(\epsilon)$ for ρ_W^c, in contrast to $\rho(S)$ for which it leads to a result of order $O(1)$ [3]. Hence if one computes $\rho_W(S_1,S_2) = \rho(S_1)\rho(S_2) + \rho_W^c(S_1,S_2)$ to $O(\epsilon)$ one must pay attention to the fact that $\rho_W^c(S_1,S_2)$ can be computed using the improved-tree theory, but $\rho(S)$ has then to be computed to one-loop accuracy. In the same way, the connected generating function

$$Z_W^c(\lambda_1,\lambda_2) = Z_W(\lambda_1,\lambda_2) - Z(\lambda_1)Z(\lambda_2) \quad (60)$$

can be computed exactly up to order $O(\epsilon)$ using the improved tree theory, but to compute $Z_W(\lambda_1,\lambda_2)$ up to order ϵ one must add one-loop corrections to $Z(\lambda)$. The same remark holds for the moments $\langle S_1^{n_1}S_2^{n_2}\rangle_{\rho_W^c} = \langle S_1^{n_1}S_2^{n_2}\rangle_{\rho_W} - \langle S_1^{n_1}\rangle_\rho \langle S_2^{n_2}\rangle_\rho$.

[3] To be rigorous, this is only true of the dimensionless density $\tilde{\rho}(\tilde{S}) = S_m^2\rho(S_m\tilde{S})$ since $S_m = O(\epsilon)$, we neglect this subtlety in the following.

IV. CORRELATIONS BETWEEN TOTAL SHOCK SIZES

A. Reminder of the diagrammatic rules and extraction of shock moments

Let us now explain how the moments

$$\begin{aligned} & C^{(n,m)}(w_1,\dots,w_n,w_{n+1},\dots,w_{n+m}) \\ &= L^{(n+m-2)d}\overline{\hat{u}(w_1)\dots\hat{u}(w_n)\hat{u}(w_{n+1})\dots\hat{u}(w_{n+m})} \\ &= L^{-2d}\int_{y_1\dots y_{n+m}} \overline{\hat{u}_{y_1}(w_1)\dots\hat{u}_{y_{n+m}}(w_{n+m})} \end{aligned} \tag{61}$$

are obtained using the diagrammatic rules developed in Ref. [31] which can also be read off from the action (57). In the calculation of the correlator (54), the terms of the form $L^d\hat{u}(w_i)=\int_{y_i}\hat{u}_{y_i}(w_i)$ are diagrammatically represented as external legs at the top of the diagrams. Fields at different position w_i and w_j can be contracted through an interaction vertex $\int_z \frac{1}{T^2}R(\hat{u}_z(w_i)-\hat{u}_z(w_j)+w_i-w_j)$, represented as a dashed-line (each contraction bringing an additional derivative to R with the appropriate sign). The propagators are represented as plain lines. When forming tree diagrams, one produces $n+m-1$ interaction vertices $\frac{1}{T^2}R$, and $2(n+m-1)$ propagators, which each carries a factor of T. For trees, all factors of T cancel, and the diagrams survive in the 0 temperature limit. The factors of T can thus be omitted in the diagrammatic rules. As for the integrals over the positions of the external legs y_i, $i=1,\dots,n+m$ and the disorder vertices z_k, $k=1,\dots,n+m-1$, since the interaction is local in space and $\int_x g_x=\frac{1}{m^2}$, all $2(n+m-1)$ propagators can be taken as static propagators and thus this integration produces an additional factor of L^d. This procedure results in expressions for the $C^{(n,m)}(w_1,\dots,w_n,w_{n+1},\dots,w_{n+m})$ as sums of products of terms involving derivatives $\Delta^{(p)}(w_i-w_j)$ [4]. In calculating the Kolmogorov cumulants $K^{(n,m)}(\delta_1,\delta_2)$ to order $O(\delta_1\delta_2)$ one must use the even but non-analytic form of $\Delta(u)$ around the origin,

$$\Delta(u)=\Delta(0)+\Delta'(0^+)|u|+\frac{\Delta''(0)}{2}u^2+O(u^3)\ . \tag{62}$$

We checked that if one takes all limits of coinciding points with a fixed order of the w_i in the calculation, one obtains a non-ambiguous result, independent of the ordering.

B. Lowest moments

First moment: We fist consider the computation of $\langle S_1S_2\rangle^{\rm c}_{\rho_W}$. To this aim we compute $C^{(1,1)}(w_1,w_2)$, which is given by a single diagram:

$$C^{(1,1)}(w_1,w_2) \;=\; \underset{\frac{1}{m^2}}{w_1\approx 0}\ \underset{\Delta(w_1-w_2)}{}\ \underset{\frac{1}{m^2}}{w_2\approx W} \;=\; \frac{1}{L^dm^4}\Delta(w_1-w_2)\ . \tag{63}$$

We have introduced a new diagrammatic notation: A double-dashed line represents an interaction vertex between position fields at a finite distance $\approx W$; we reserve the single dashed line for interaction vertices between nearby position fields. Hence,

$$\begin{aligned} K^{(1,1)}_W(\delta_1,\delta_2) &= \frac{1}{L^dm^4}\Big[\Delta(-\delta_1+W+\delta_2)-\Delta(W+\delta_2) \\ &\qquad -\Delta(-\delta_1+W)+\Delta(W)\Big] \\ &= -\frac{\Delta''(W)}{L^dm^4}\delta_1\delta_2+O(\delta_i^2)\ . \end{aligned} \tag{64}$$

Using (53) we conclude that

$$L^{-2d}\langle S_1S_2\rangle^{\rm c}_{\rho_W}=-\frac{\Delta''(W)}{L^dm^4}\ . \tag{65}$$

This is the exact result (40), here retrieved diagrammatically within the improved tree approximation. A priori there could be higher-order corrections $O(\epsilon^2)$ on the r.h.s. of (65), coming from loop diagrams. However, the definition (23) of $\Delta(u)$ as a physical observable effectively resums an infinite number of loop diagrams. The same diagrams then arise on both sides of Eq. (65), and the result (40) is exact.

Second moment: Let us now consider the computation of $\langle S_1^2S_2\rangle^{\rm c}_{\rho_W}$. We first need to compute $C^{(2,1)}(w_1,w_2,w_3)$. Diagramamtically it is given by

$$C^{(2,1)}(w_1,w_2,w_3)$$

$$= 2\,{\rm Sym}_{w_1\leftrightarrow w_2}\Big(\underset{w_2\approx 0}{}\ \underset{w_1\approx 0}{}\ \underset{w_3\approx W}{} \;+\; \underset{w_3\approx W}{}\ \underset{w_1\approx 0}{}\ \underset{w_2\approx 0}{} \;+\; \underset{w_2\approx 0}{}\ \underset{w_3\approx W}{}\ \underset{w_1\approx 0}{} \Big)$$

$$= \frac{2}{L^dm^8}{\rm Sym}_{w_1\leftrightarrow w_2}\Big[\Delta(w_1-w_2)\Delta'(w_1-w_3)+\Delta(w_1-w_3)\Delta'(w_1-w_2)+\Delta(w_3-w_2)\Delta'(w_3-w_1)\Big] \tag{66}$$

In doing the $\mathcal{K}$ operation to go from $C^{(2,1)}$ to $K_W^{(2,1)}$, these diagrams are not equivalent. At order $\delta_1\delta_2$ that we are interested in, the first term leads to $4\frac{\Delta'(0^+)}{m^4}\frac{\Delta''(W)}{L^d m^4}\delta_1\delta_2$, the second to $2\frac{\Delta'(0^+)}{m^4}\frac{\Delta''(W)}{L^d m^4}\delta_1\delta_2$, whereas the third one is of order $O(\delta_1^2\delta_2)$ and does not contribute. Using Eq. (53) we conclude that

$$L^{-2d}\langle S_1^2 S_2\rangle_{\rho_W^c} = 6\frac{\Delta'(0^+)}{m^4}\frac{\Delta''(W)}{L^d m^4} + O(\epsilon^2)\ . \qquad (67)$$

General rules for diagrams: The last example is rather instructive for the three general rules:

(i) the only diagrams that contribute to the Kolmogorov cumulant $K_W^{(n,m)}(\delta_1,\delta_2)$ at order $\delta_1\delta_2$ contain a single double-dashed vertex (that is a single disorder interaction vertex connecting the two disjoint sets of points at $w\approx 0$ and $w\approx W$);

(ii) this vertex becomes a $\Delta''(W)$ at order $\delta_1\delta_2$;

(iii) the other interaction vertices are between (almost) coinciding points, and produce a factor of $\Delta'(0^+)$ at order $\delta_1\delta_2$. These rules are discussed in Appendix B. As a result, diagrams contributing to the two-shock moments consist of diagrams reminiscent of the one-shock case (i.e. they contain only $\Delta'(0^+)$ vertices) linked together by an interaction vertex $-\frac{\Delta''(W)}{L^d m^4}$.

C. Generating function for all moments

Let us now use the above rules and give a diagrammatic computation of $Z_W^c(\lambda_1,\lambda_2) = \hat{Z}_W^c(\lambda_1,\lambda_2)$ defined in Eq. (48). To this aim, let us first introduce a diagrammatic notation for $Z(\lambda)$ defined in Eq. (43):

$Z(\lambda) =$. (68)

We have emphasized using dots that there is an arbitrary number of external legs at the top of the diagrams summed in Eq. (68). Using the expansion (49) and following the rules explained in the previous section, the diagrams entering in $\hat{Z}_W^c(\lambda_1,\lambda_2)$ are made of two trees linked by a single doubled dashed line. It is the sum of all tree diagrams for avalanches at $w=0$, times all tree diagrams for avalanches at $w=W$, linked together by a single $-\frac{\Delta''(W)}{L^d m^4}$ inserted between any pair of points belonging to each tree. This can be represented as

$Z_W^c(\lambda_1,\lambda_2) = \hat{Z}_W^c(\lambda_1,\lambda_2)$

$=$ 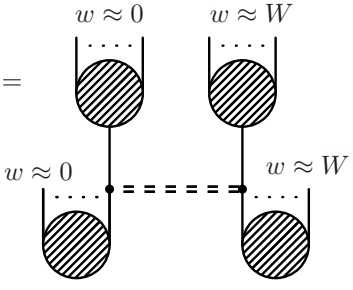

. (69)

The diagrams above the point of insertion of $\Delta''(W)$ on the left are given by $Z(\lambda_1)$. The terms below are all the diagrams in $Z(\lambda_1)$ with an arbitrary external leg selected, that is $\frac{dZ(\lambda_1)}{d\lambda_1}$. A similar contribution arises on the right-hand side. Hence we arrive at the result

$$Z_W^c(\lambda_1,\lambda_2) = -\frac{\Delta''(W)}{L^d m^4} Z(\lambda_1)\frac{dZ(\lambda_1)}{d\lambda_1} Z(\lambda_2)\frac{dZ(\lambda_2)}{d\lambda_2} + O(\epsilon^2) \qquad (70)$$

In terms of $Z_W(\lambda_1,\lambda_2)$ this result reads

$$Z_W(\lambda_1,\lambda_2) = Z(\lambda_1)Z(\lambda_2) - \frac{\Delta''(W)}{L^d m^4} Z(\lambda_1)\frac{dZ(\lambda_1)}{d\lambda_1} Z(\lambda_2)\frac{dZ(\lambda_2)}{d\lambda_2}\ . \qquad (71)$$

It is correct to $O(\epsilon)$ if one takes into account the $O(\epsilon)$ corrections to $Z(\lambda)$. Expanding the result (70) one obtains the moments $\langle S_1^n S_2^m\rangle_{\rho_W^c}$:

$$\langle S_1^n S_2^m\rangle_{\rho_W^c} = -\frac{\Delta''(W)}{L^{3d} m^4} n!m! \times \sum_{p=0}^{n-1}\sum_{q=0}^{m-1} \frac{\langle S^{n-p}\rangle_\rho \langle S^{p+1}\rangle_\rho \langle S^{m-q}\rangle_\rho \langle S^{q+1}\rangle_\rho}{(n-p)!p!(m-q)!q!} + O(\epsilon^2)\ . \qquad (72)$$

The diagrammatic interpretation of this result is straightforward: to construct an arbitrary diagram contributing to $\langle S_1^n S_2^m\rangle_{\rho_W^c}$, one must first choose $p\le n-1$ external legs on the left that will be below the point of insertion of $-\frac{\Delta''(W)}{L^d m^4}$ (there must be at least one leg above this point of insertion). In the $\mathcal{K}$ operation, all those points lead to a term that contributes to $\langle S^p\rangle_\rho$. The combinatorial term accounts for the C_p^n possible choices. Note that this result was derived using the heuristic diagrammatic rules developed in the preceding section. We observe that:

(i) It correctly reproduces the results for the small-order moments (65) and (67). We checked that it leads to $\langle S_1^3 S_2\rangle_{\rho_W^c} = -60\frac{\Delta''(W)}{L^d m^4} S_m^2$ and $\langle S_1^2 S_2^2\rangle_{\rho_W^c} = -27\frac{\Delta''(W)}{L^d m^4} S_m^2$, which can also be derived from the expression for $\hat{C}^{(4)}(w_1,w_2,w_3,w_4)$ given e.g. in formula (61) of Ref. [31].

(ii) We give in Appendix C an alternative derivation of Eq. (71) that uses the Carraro-Duchon formalism [32, 42].

(iii) We give in Appendix D a derivation using a saddle-point calculation within the effective action (57). This also yields the local structure of correlations studied in Section V.

D. Results for the densities

To infer ρ_W from Eq. (71), we first note the identity $Z(\lambda)\frac{dZ(\lambda)}{d\lambda} = \frac{1}{2S_m}\frac{d}{d\lambda}\left(Z(\lambda)-\lambda\right)$, derived from the self-consistent equation (58) for $Z(\lambda)$. Differentiating $L^{-d}\int dS(e^{\lambda S}-1)\rho(S) = Z(\lambda)$ with respect to λ and using $\langle S\rangle_\rho = L^d$ yields

$$L^{-d}\int dS(e^{\lambda S}-1)S\rho(S) = \frac{d}{d\lambda}\left[Z(\lambda)-\lambda\right]\ . \qquad (73)$$

Finally, using Eqs. (45) and (71), we obtain

$$\rho_W(S_1,S_2) = \rho(S_1)\rho(S_2)\left(1 - \frac{\Delta''(W)}{L^d m^4}\frac{S_1 S_2}{4S_m^2}\right) . \quad (74)$$

This is our main result for the two-schock density, already announced in Eq. (10) of the introduction. It can be used to extract a variety of physical observables.

Mean number of pairs of shocks: Integrating over S_1 and S_2, we obtain two equivalent formulas for $\rho_2(W)$:

$$\begin{aligned}\rho_2(W) &= \rho_0^2 - \frac{\Delta''(W)}{L^d m^4}\frac{L^{2d}}{4S_m^2} \quad (75)\\ &= \rho_0^2\left[1 - \frac{\Delta''(W)}{L^d m^4}\left(\frac{\langle S\rangle_P}{2S_m}\right)^2\right] .\end{aligned}$$

Hence, although both ρ_0 and $\rho_2(W)$ are non-universal and dominated by the non-universal small avalanche size cutoff S_0 discussed in Sec. III E, the connected density $\rho_2(W) - \rho_0^2$ does not depend on S_0 and is universal.

Normalized probability distribution: The above results allow us to express the probability distribution $P_W(S_1,S_2) = \frac{\rho_W(S_1,S_2)}{\rho_2(W)}$ to $O(\epsilon)$ accuracy as

$$P_W(S_1,S_2) = P(S_1)P(S_2)\left[1 - \frac{\Delta''(W)}{4S_m^2 L^d m^4}\Big(S_1S_2 - \langle S\rangle_P^2\Big)\right] . \quad (76)$$

Conditional probability distribution: Another PDF of interest is the conditional probability to have a shock with amplitude S_2, given that there was a shock of amplitude S_1 at a distance W before. To $O(\epsilon)$ accuracy

$$\begin{aligned}P_W(S_2|S_1) &= \frac{P_W(S_1,S_2)}{\int dS_2 P_W(S_1,S_2)} \quad (77)\\ &= P(S_2)\left[1 - \frac{\Delta''(W)S_1}{4S_m^2 L^d m^4}\Big(S_2 - \langle S\rangle_P\Big)\right] .\end{aligned}$$

Its mean value, normalized by $\langle S\rangle_P$, is

$$\frac{\langle S_2|S_1\rangle}{\langle S\rangle_P} = 1 - \frac{\Delta''(W)S_1}{4S_m^2 L^d m^4}\Big(2S_m - \langle S\rangle_P\Big) . \quad (78)$$

Second shock marginal: The probability for the size S_2 of a second shock at W, given that there was a shock at 0, is

$$\begin{aligned}P_W(S_2) &= \int dS_1 P_W(S_1,S_2)\\ &= P(S_2)\left[1 - \frac{\Delta''(W)\langle S\rangle_P}{4S_m^2 L^d m^4}\Big(S_2 - \langle S\rangle_P\Big)\right] .\end{aligned} \quad (79)$$

The normalized mean value of the second shock is

$$\frac{\langle S_2\rangle_W}{\langle S\rangle_P} = 1 - \frac{\Delta''(W)\langle S\rangle_P}{4S_m^2 L^d m^4}\Big(2S_m - \langle S\rangle_P\Big) . \quad (80)$$

E. Analysis of the results

Sign of the correlations: As discussed in Sec. III C, the sign of the correlations (positively or negatively correlated shock sizes) solely depends on the sign of $\Delta''(W)$, which depends on the distance W and on the universality class of the problem. The above results thus unveil a rich phenomenology for the correlations as pictured in Fig. 1.

Range of validity: The result (70) was obtained in the framework of the ϵ expansion. The results for the connected part of the correlations are by definition the first non-zero terms in this expansion, since they were obtained within the improved tree approximation, and they appear at $O(\epsilon)$. As a perturbative result, it is by definition controlled for $\epsilon \to 0$. For finite ϵ, the predictions should be accurate as long as the corrections to the mean-field behavior are small. This is worth emphasizing, since the moments $\langle S_1^n S_2^m\rangle_{\rho_W}$ predicted by the formula (72) become negative for large (n,m), signaling a breakdown of the improved tree approximation. This is also the case of the two-shock density computed at the improved tree level in Eq. (74) which becomes negative at large S_i. There the approximation is not controlled anymore since $O(\epsilon)$ corrections are larger than the mean-field result. Let us see when this occurs: Using the simple estimate $\Delta''(W) \approx |\Delta'(0^+)|/W_\mu$, where W_μ is the length of order $\mu^{-\zeta}$ on which $\Delta(W)$ decays, see below, and $|\Delta'(0^+)| = m^4 S_m$, the bound $\rho(S_1,S_2) > 0$ is violated if

$$1 \lesssim \frac{S_m}{W_\mu \mu^{-d}} \times \frac{1}{(\mu L)^d} \times \frac{S_1 S_2}{4S_m^2} . \quad (81)$$

The first factor is a dimensionless number of order $O(\epsilon)$ near $d = d_{\rm uc}$. The second vanishes in the thermodynamic limit of $L \to \infty$. Thus the bound can only be violated if S_1S_2/S_m^2 compensates this factor. This can only be achieved if at least one of the avalanches is either system-spanning, or far out in the tail of the distribution, i.e. the bound is only violated for very unlikely events.

Note however that the exact result (40) is protected from being negative since

$$L^{-2d}\langle S_1 S_2\rangle_{\rho_W} = 1 - \frac{\Delta''(W)}{L^d m^4} = \overline{\partial_w u(w)\partial_w u(W+w)} , \quad (82)$$

and $\partial_w u(w)$ is always positive since $u(w)$ is monotonically increasing as a function of w. The latter can be shown rigorously using a stability argument: Writing that $u_x(w)$ is a stable minimum of the Hamiltonian (14) implies for all x two equations, namely $\frac{\delta\mathcal{H}[u,w]}{\delta u(x)} = 0$, and $\frac{\delta^2\mathcal{H}[u,w]}{\delta u(x)\delta u(y)} \geq 0$. Specifying the second equation to $x = y$, we obtain

$$m^2[u_x(w) - w] + \partial_u V(u_x(w),x) = 0 , \quad (83)$$

$$m^2 + \partial_u^2 V(u_x(w),x) \geq 0. \quad (84)$$

Taking a derivative of Eq. (83) w.r.t. w, solving for $\partial_w u_x(w)$, and using Eq. (84) implies

$$\partial_w u_x(w) = \frac{1}{1 + m^{-2}\partial_u^2 V(u_x(w),x)} \geq 0 . \quad (85)$$

Comparison with experiments and numerics: Though our predictions rely on the analysis of the model (14), they were obtained using FRG and thus we expect Eqs. (70) and (72) to be valid for all models in the same universality class. All our results, namely Eq. (72) and Eqs. (74)-(80), contain the combination $\frac{\Delta''(W)}{L^d m^4}$. On one hand it can be used to give a result to order $O(\epsilon)$ in the form of a universal function (see below). On the other hand all quantities entering the r.h.s of these equations can be measured directly in an experiment or in a numerical simulation. Indeed we recall that

$$S_m := \frac{\langle S^2\rangle_P}{2\langle S\rangle_P} \equiv \frac{\langle S^2\rangle_\rho}{2\langle S\rangle_\rho} \tag{86}$$

and the combination

$$\frac{\Delta''(W)}{L^d m^4} = \partial_W^2 \overline{[u(w)-w][u(w+W)-w-W]}^c \tag{87}$$

can both be measured and do not require to know the mass m which might be hard to identify. The computation of this second derivative then gives a precise characterization of the amplitude of the correlations through the exact formula (41). The accuracy of the ϵ expansion and universality can then be tested against the formulas given in the previous section.

Universal function: Using rescaled quantities we can rewrite our main result as (see Eq. (24) and Sec. III C)

$$\rho^c_W(S_1,S_2) = \frac{1}{(L\mu)^d}\frac{L^{2d}}{S_m^4}\mathcal{F}_d\Big(\frac{W}{W_\mu},\frac{S_1}{S_m},\frac{S_2}{S_m}\Big) \tag{88}$$

where the function $\mathcal{F}_d$ is universal and depends only on the space dimension. To first order in $d = d_{\rm uc} - \epsilon$, it is given by

$$\mathcal{F}(w,s_1,s_2) \simeq \frac{A_d \Delta^{*\prime\prime}(w)}{16\pi\sqrt{s_1 s_2}} e^{-(s_1+s_2)/4} + O(\epsilon^2) \tag{89}$$

in the limit of large L and small μ and A_d was given in Eq. (25). Here $\Delta^{*\prime\prime}(w)$ is the universal fixed point of the FRG equation, normalized to $\Delta^*(0) = \epsilon$. Indeed, for small m the rescaled renormalized disorder correlator of the system $\tilde\Delta(w)$, appearing in Eq. (24), is close to one of the fixed points of the FRG equation: $\tilde\Delta(w) \simeq \tilde\Delta^*(w)$. For non-periodic disorder, the latter can be expressed using one constant κ as $\tilde\Delta^*(w) = \kappa^2\Delta^*(w/\kappa)$ (see Sec. III C). The parameter κ is thus the single non-universal constant in our formula. The scales in Eq. (88) are then given by

$$W_\mu \simeq \kappa\mu^{-\zeta}\ , \qquad S_m \simeq A_d\kappa\Delta^{*\prime}(0^+)\mu^{-(d+\zeta)} \tag{90}$$

for small μ. We remind that $m = \mu^{\gamma/2}$. We have defined all quantities such that their expressions are the most simple ones, independent of γ. With the above normalization, to order ϵ, $\Delta^{*\prime}(0^+) = \sqrt{\epsilon(\epsilon-2\zeta)}$ and $\Delta^{*\prime\prime}(0) = \frac{2\epsilon}{9}$.

Locality: Note that in the result (88) the amplitude of the correlation is inversely proportional to $N = (L\mu)^d$, the number of elastically independent degrees of freedom of the interface. This is a signature of the local nature of the correlations. For two shocks a distance W apart, there is a probability of order $1/N$ that they occur in the same region of space. To go further into this locality property and to remove this bias we investigate in the next section the correlations between the local shock sizes.

V. LOCAL STRUCTURE OF CORRELATIONS

In this section we analyze the correlations between the local shock sizes. We start by deriving a general formula for the correlations between the local shock sizes measured on an arbitrary subset of the internal space of the interface. To this aim we define

$$S_1^{\phi_1} = \int_x S_{1x}\phi_{1x}\ , \qquad S_2^{\phi_2} = \int_x S_{2x}\phi_{2x}\ , \tag{91}$$

where ϕ_1 and ϕ_2 are two arbitrary test functions. Two extreme cases are $\phi_{1x} = 1$: in this case $S_1^{\phi_1} = S_1$, and the observable is the total size studied in the precedent section. The other extreme is $\phi_{1x} = \delta^d(x-x_1)$, for which $S_1^{\phi_1} = S_{1x_1}$ is the local size at $x = x_1$.

A. Reminder: one-shock case

Here we briefly recall the essential definitions and results given in Refs. [31, 32] on the density and generating function associated to the local one-shock size statistics. For a general test function ϕ we introduce

$$\begin{aligned}
\rho^\phi(S^\phi) &:= \overline{\sum_i \delta(S^{(i),\phi}-S^\phi)\delta(w_i-w)}\ ,\\
Z^\phi(\lambda) &:= \frac{1}{\int_x\phi_x}\langle e^{\lambda S^\phi}-1\rangle_{\rho^\phi}\ ,\\
\hat Z^\phi(\lambda) &:= Z^\phi(\lambda)-\lambda\ ,
\end{aligned} \tag{92}$$

where $\langle ...\rangle_{\rho^\phi}$ denotes the average with respect to ρ^ϕ. Note that $\hat Z^\phi$ has no linear term, since the first moment of ρ^ϕ is due to STS

$$\langle S^\phi\rangle_{\rho^\phi} = \int_x \phi_x\ . \tag{93}$$

The generating function $\hat Z^\phi(\lambda)$ is obtained from the replica field theory using the exact relation

$$\hat Z^\phi(\lambda) = \frac{1}{\int_x\phi_x}\partial_\delta \overline{e^{\int_x \phi_x[u_x(w+\delta)-u_x(w)-\delta]}}|_{\delta=0^+}\ . \tag{94}$$

It was shown in Refs. [31, 32] that $Z^\phi(\lambda)$ can be written as

$$Z^\phi(\lambda) = \frac{\int_x Z_x^\phi(\lambda)}{\int_x\phi_x}\ , \tag{95}$$

where, at the improved-tree-theory level, $Z_x^\phi(\lambda)$ satisfies the following self-consistent equation

$$Z_x^\phi(\lambda) = \lambda\phi_x + \sigma \int_{yy'} g_{x-y} g_{x-y'} Z_y^\phi(\lambda) Z_{y'}^\phi(\lambda) \ . \qquad (96)$$

The quantity $\sigma = -\Delta'(0^+)$ was defined in Eq. (38).

B. Two-shock case: Notation and diagrammatic result

Densities and generating functions: Consider

$$\rho_W^{\phi^1\phi^2}(S_1^{\phi^1}, S_2^{\phi^2}) := \overline{\sum_{i\neq j} \delta(w-w_i)\delta(S_1^{\phi^1} - S^{(i),\phi^1})\delta(w+W-w_j)\delta(S_2^{\phi^2} - S^{(j),\phi^2})} \ .$$

The generating functions are

$$Z_W^{\phi^1\phi^2} := \frac{1}{\int_x \phi_x^1 \int_x \phi_x^2} \left\langle \left(e^{\lambda_1 S_1^{\phi^1}} - 1\right)\left(e^{\lambda_2 S_2^{\phi^2}} - 1\right)\right\rangle_{\rho_W^{\phi^1\phi^2}} \qquad (97)$$

$$\hat{Z}_{w_2-w_1}^{\phi^1\phi^2}(\lambda_1,\lambda_2) := \frac{1}{\int_x \phi_x^1 \int_x \phi_x^2} \lim_{\delta_1,\delta_2\to 0^+} \partial_{\delta_1,\delta_2} \overline{e^{\int_x \phi_x^1 \lambda_1 [\hat{u}_x(w_1+\delta_1)-\hat{u}_x(w_1)]} e^{\int_x \phi_x^2 \lambda_2 [\hat{u}_x(w_2+\delta_2)-\hat{u}_x(w_2)]}} \ , \qquad (98)$$

where $\langle ... \rangle_{\rho_W^{\phi^1\phi^2}}$ denotes the average with respect to $\rho_W^{\phi^1\phi^2}$. The following relation holds

$$\begin{aligned} Z_W^{\phi^1\phi^2}(\lambda_1,\lambda_2) \ &= \ \hat{Z}_W^{\phi^1\phi^2}(\lambda_1,\lambda_2) + Z^{\phi^1}(\lambda_1)\lambda_2 \\ &\quad + \lambda_1 Z^{\phi^2}(\lambda_2) - \lambda_1\lambda_2 \ . \end{aligned} \qquad (99)$$

(These relations are a consequence of Appendix A). The connected equivalents of the previous definitions are constructed as in the previous section for the correlations between the total sizes; for example

$$\rho_W^{c;\phi^1\phi^2}(S_1^{\phi^1}, S_2^{\phi^2}) = \rho_W^{\phi^1\phi^2}(S_1^{\phi^1}, S_2^{\phi^2}) - \rho^{\phi^1}(S_1^{\phi^1})\rho^{\phi^2}(S_2^{\phi^2}), \qquad (100)$$

and we note $\langle ... \rangle_{\rho_W^{c;\phi^1\phi^2}}$ the average w.r.t. $\rho_W^{c;\phi^1\phi^2}$.

Simplified notation for averages: In order that these somewhat complicated notations do not obscure our results, we introduce simplified notations for averages. We first note that

$$\rho_W^{\phi^1\phi^2}(S_1^{\phi^1}, S_2^{\phi^2}) = \rho_2(W)\mathcal{P}(S_1^{\phi^1}, S_2^{\phi^2}), \qquad (101)$$

where $\rho_2(W)$ is as before the density of a pair of shocks and $\mathcal{P}(S_1^{\phi^1}, S_2^{\phi^2})$ denotes the probability, given that two shocks occured at a distance W, that their local sizes measured with respect to ϕ^1 and ϕ^2 are $S_1^{\phi^1}$ and $S_2^{\phi^2}$. We have dropped the dependence of $\mathcal{P}$ on ϕ^1 and ϕ^2 to alleviate our notations. We also note arbitrary moments as

$$\langle\langle (S_1^{\phi 1})^n (S_2^{\phi^2})^m \rangle\rangle_{\rho_W} \ := \ \langle (S_1^{\phi 1})^n (S_2^{\phi^2})^m \rangle_{\rho_W^{\phi^1\phi^2}} \qquad (102)$$

$$\langle\langle (S_1^{\phi 1})^n (S_2^{\phi^2})^m \rangle\rangle_{\rho_W^c} \ := \ \langle (S_1^{\phi 1})^n (S_2^{\phi^2})^m \rangle_{\rho_W^{c;\phi^1\phi^2}}. \qquad (103)$$

We indicate the dependence on the choice of ϕ^1 and ϕ^2 only inside the average, and not in the measure. A moment of the form $\langle\langle (S_1^{\phi 1})^n (S_2^{\phi^2})^m \rangle\rangle_{\rho_W}$ is thus equal to the product of $\rho_2(W)$ and of the mean value of $(S_1^{\phi 1})^n (S_2^{\phi^2})^m$ for shocks at a distance W, given that two such shocks occurred.

Diagrammatic result: In Appendix D we compute these generating functions by a direct evaluation of Eq. (97) using a saddle-point calculation on the effective action (57). Alternatively, from a diagrammatic point of view, the result can be adapted from the reasoning that led to $Z_W(\lambda_1,\lambda_2)$ by *keeping track of the space dependence in the different vertices, propagators and sources in the diagram* (69). Following Eq. (68), we represent $Z_x^\phi(\lambda)$ as

$$Z_x^\phi(\lambda) = \qquad . \qquad (104)$$

The same diagram without the marked point x is also used to represent $\int_x Z_x^\phi(\lambda)$, itself equal to $\int_x \phi_x \times Z^\phi(\lambda)$. Then, as before, $\hat{Z}_W^{\phi^1\phi^2}(\lambda_1,\lambda_2)$ is the sum of a connected and a disconnected part:

$$\hat{Z}_W^{\phi^1\phi^2}(\lambda_1,\lambda_2) = \hat{Z}^{\phi^1}(\lambda_1)\hat{Z}^{\phi^2}(\lambda_2) + \hat{Z}_W^{c,\phi^1\phi^2}(\lambda_1,\lambda_2) \ . \qquad (105)$$

The connected part $\hat{Z}_W^{c;\phi^1\phi^2}(\lambda_1,\lambda_2)$ is

$$\hat{Z}_W^{c;\phi^1\phi^2}(\lambda_1,\lambda_2) \qquad \phi_1; w\approx 0 \qquad \phi_2; w\approx W$$
$$= \frac{1}{\int_x \phi_x^1 \int_x \phi_x^2} \times \tag{106}$$

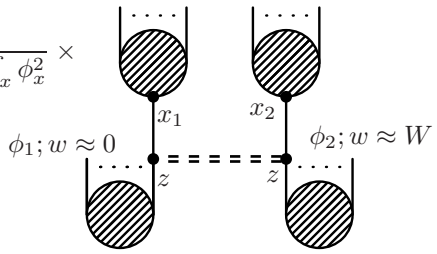

It can be written as

$$\hat{Z}_W^{c,\phi^1\phi^2}(\lambda_1,\lambda_2) = -\frac{\Delta''(W)}{\int_x \phi_x^1 \int_x \phi_x^2}$$
$$\int_{zx_1x_2y_1y_2} g_{zx_1} Z_{x_1}^{\phi^1}(\lambda_1) \frac{\delta Z_{y_1}^{\phi^1}(\lambda_1)}{\lambda_1 \delta\phi_z^1} g_{zx_2} Z_{x_2}^{\phi^2}(\lambda_2) \frac{\delta Z_{y_2}^{\phi^2}(\lambda_2)}{\lambda_2 \delta\phi_z^2}$$
$$+O(\epsilon^2)\ . \tag{107}$$

We note that it is possible to obtain a more explicit formula for avalanches measured on parallel hyperplanes, see Appendix D 2. In the next section we focus on the first moments which already contain valuable information.

C. First moments: arbitrary sources and kernels

The first moments of $\rho_W^{c;\phi^1\phi^2}$ are obtained from the combination of Eqs. (97), (99), (105) and (107). One first needs the series expansion for $Z_x^\phi(\lambda)$. It is obtained from Eq. (96) at arbitrary order in λ; here we give it up to order 3:

$$Z_x^\phi(\lambda) = \lambda\phi_x + \lambda^2\sigma \int_{yy'} g_{x-y} g_{x-y'} \phi_y \phi_{y'} \tag{108}$$
$$+2\lambda^3\sigma^2 \int_{yy'zz'} g_{x-y} g_{x-y'} g_{y-z} g_{y-z'} \phi_z \phi_{z'} \phi_{y'} + O(\lambda^4)$$

Hence

$$\frac{\delta Z_x^\phi}{\lambda \delta\phi_u} = \delta(x-u) + 2\lambda\sigma \int_y g_{x-y} g_{x-u} \phi_y$$
$$+2\lambda^2\sigma^2 \left(2\int_{yy'z} g_{x-y} g_{x-y'} g_{y-z} g_{y-u} \phi_z \phi_{y'} \right.$$
$$\left. + \int_{yzz'} g_{x-y} g_{x-u} g_{y-z} g_{y-z'} \phi_z \phi_{z'} \right) + O(\lambda^3)\ . \tag{109}$$

We then obtain from Eq. (107) the local version of the exact result (8), namely [5]

$$\frac{\langle\langle S_1^{\phi^1} S_2^{\phi^2}\rangle\rangle_{\rho_W^c}}{\int_x \phi_x^1 \int_x \phi_x^2} = -\frac{\Delta''(W)}{\int_x \phi_x^1 \int_x \phi_x^2} \int_{zx_1x_2} g_{z-x_1} g_{z-x_2} \phi_{x_1}^1 \phi_{x_2}^2$$
$$+O(\epsilon^2)\ . \tag{110}$$

Let us also give the result for the third-order moment,

$$\frac{\langle\langle (S_1^{\phi^1})^2 S_2^{\phi^2}\rangle\rangle_{\rho_W^c}^c}{\int_x \phi_x^1 \int_x \phi_x^2} = -\frac{\Delta''(W)}{\int_x \phi_x^1 \int_x \phi_x^2}\sigma \times$$
$$\left(4\int_{zx_1x_2y_1t_1} g_{z-x_1} g_{z-x_2} g_{y_1-t_1} g_{y_1-z} \phi_{x_1}^1 \phi_{t_1}^1 \phi_{x_2}^2 \right.$$
$$\left. +2\int_{zx_1x_2t_1t_1'} g_{z-x_1} g_{z-x_2} g_{x_1-t_1} g_{x_1-t_1'} \phi_{t_1}^1 \phi_{t_1'}^1 \phi_{x_2}^2 \right)$$
$$+O(\epsilon^2)\ . \tag{111}$$

D. First moment: correlations between the local shock sizes for short-ranged elasticity.

Let us now give the precise form of the first connected moment for an interface with the short-ranged elasticity (15) and for correlations between the local avalanche sizes at two points x_1 and x_2. We choose $\phi_x^1 = \delta^d(x-x_1)$ and $\phi_x^2 = \delta^d(x-x_2)$ and note $x = |x_1 - x_2|$ the distance between the two points. Thus $S_1^{\phi^1} = S_{1x_1}$ and $S_2^{\phi^2} = S_{2x_2}$. We obtain

$$\langle\langle S_{1x_1} S_{2x_2}\rangle\rangle_{\rho_W^c} = -\Delta''(W) \int_q e^{iq(x_1-x_2)} g_q g_{-q}$$
$$= -\Delta''(W) m^{d-4} 2^{-\frac{d}{2}-1} \pi^{-\frac{d}{2}} (mx)^{2-\frac{d}{2}} K_{2-\frac{d}{2}}(mx)$$
$$=_{x=0} -\Delta''(W) 2^{-d} \pi^{-\frac{d}{2}} m^{d-4} \Gamma\left(2-\frac{d}{2}\right)$$
$$\simeq_{x\gg 1/m} -\Delta''(W) 2^{-\frac{d}{2}-\frac{3}{2}} \pi^{\frac{1}{2}-\frac{d}{2}} m^{\frac{d-5}{2}} x^{\frac{3}{2}-\frac{d}{2}} e^{-mx}\ , \tag{112}$$

where $K_n(x)$ denotes a modified Bessel function of the second kind. Note that integrating this formula yields an exact result,

$$\int_{x_1,x_2} \langle\langle S_{1x_1} S_{2x_2}\rangle\rangle_{\rho_W^c} = \langle S_1 S_2\rangle_{\rho_W^c} = -L^d \frac{\Delta''(W)}{m^4}\ . \tag{113}$$

This is equivalent to Eq. (41), which is *exact*. We thus expect Eq. (112) to be quite accurate even for large values of ϵ.

[5] The result (110) can simply be turned into an exact one if one introduces the bi-local part of the renormalized disorder correlator $\Delta_{x_2-x_1}(w_1-w_2) = m^4\overline{[u_{x_1}(w_1)-w_1][u_{x_2}(w_2)-w_2]}$ (see also [41]) and proceeds as in Sec. III F. The result (110) can then be understood as the lowest-order approximation of $\Delta_{x_2-x_1}(w)$ in terms of $\Delta(w)$.

As expected, we observe that the amplitude of the correlations decays exponentially beyond the length $L_m = 1/m$. For smaller distances they decay algebraically with an exponent that depends on the dimension:

$$\begin{aligned}
&\langle\langle S_{1x_1} S_{2x_1+x}\rangle\rangle_{\rho^c_W} - \langle\langle S_{1x_1} S_{2x_1}\rangle\rangle_{\rho^c_W} \\
&\quad \simeq_{d=1} \frac{\Delta''(W)}{8m} x^2 + O(x^3) \\
&\quad \simeq_{d=2} -\frac{\Delta''(W)}{16\pi}\Big[2\gamma_{\rm E} - 1 + 2\log(mx/2)\Big] x^2 \\
&\quad \simeq_{d=3} \frac{\Delta''(W)}{8\pi} x + O(x^2) \ . \qquad (114)
\end{aligned}$$

Finally, to emphasize the universal nature of Eq. (112), we note that it can be rewritten, using the notations of Sec. IV E and introducing a new universal scaling function $\mathcal{F}^{11}_d(w,x)$, as

$$\begin{aligned}
\langle\langle S_{1x_1} S_{2x_2}\rangle\rangle_{\rho^c_W} &= \mathcal{F}^{11}_d(\frac{W}{W_\mu}, m|x_1 - x_2|) \qquad (115) \\
\mathcal{F}^{11}_d(w,x) &= -2^{-\frac{d}{2}-1}\pi^{-\frac{d}{2}} A_d \Delta^{*\prime\prime}(w) x^{2-\frac{d}{2}} K_{2-\frac{d}{2}}(x) \\
&\quad + O(\epsilon^2) \ . \qquad (116)
\end{aligned}$$

E. First moment: correlations between the local shock sizes for long-ranged elasticity.

Let us now study the correlations between local avalanche sizes (we choose again $\phi^1_x = \delta^d(x - x_1)$ and $\phi^2_x = \delta^d(x - x_2)$ with $|x_1 - x_2| = x$) for the case of long-ranged elasticity using the kernel (16) with $\gamma = 1$. Then the result for the first connected moment is

$$\begin{aligned}
\langle\langle S_{1x_1} S_{2x_2}\rangle\rangle_{\rho^c_W} &= -\Delta''(W) \frac{\mu^{d-2}}{(2\pi)^{\frac{d}{2}}} (\mu x)^{1-\frac{d}{2}} K_{1-\frac{d}{2}}(x\mu) \\
&=_{d=1} \frac{e^{-\mu x}}{2\mu} \ . \qquad (117)
\end{aligned}$$

As the previous formula for short-ranged elasticity, this formula should be rather accurate for the experimentally relevant case of $d = 1$ (in this case $\epsilon = 1$). We again observe an exponential decay of the correlations beyond the length $L_\mu = 1/\mu$. However, here the correlations are constant at small distances, a signature of the long-range nature of the elasticity. As before, the universal nature of this result can be emphasized by introducing a universal scaling function $\mathcal{F}^{11}_{d,\rm LR}(w,y)$:

$$\begin{aligned}
&\langle\langle S_{1x_1} S_{2x_2}\rangle\rangle_{\rho^c_W} = \mathcal{F}^{11}_{d,\rm LR}\left(\frac{W}{W_\mu}, \mu|x_1 - x_2|\right) \qquad (118) \\
&\mathcal{F}^{11}_d(w,x) = -(2\pi)^{-\frac{d}{2}} A_d \Delta^{*\prime\prime}(w) x^{1-\frac{d}{2}} K_{1-\frac{d}{2}}(x) + O(\epsilon^2) \ ,
\end{aligned}$$

where we used the same notations as in Sec. IV E.

VI. MEASUREMENT OF CORRELATIONS IN SIMULATIONS OF $d = 0$ TOY MODELS.

A. Models and goals

In this section we compare our results with numerical simulations of toy models of a particle in a discrete random potential. The position of the particle can only take integer values $u \in \mathbb{N}$ and its Hamiltonian is

$$\mathcal{H}_V[u;w] = V(u) + \frac{1}{2} m^2 (u - w)^2 \ , \qquad (119)$$

where V is a random potential. We consider two distributions for the random potential mimicking the two non-periodic static universality classes of interfaces models:

RB model: The first model is a toy model for the Random-Bond universality class with short-ranged correlated disorder where the random potentials $V(i)$ at each site $i \in \mathbb{N}$, are chosen as independent, centered and normalized Gaussian random variables.

RF model: The second model is a toy model for the Random-Field universality class where $V(0) = 0$ and for $i \geq 1$, $V(i) = -\sum_{j=1}^{i} F(j)$; the random forces $F(i)$ at each site $i \in \mathbb{N}$ are chosen as independent, centered and normalized random variables. Thus $V(i)$ is a random walk with Gaussian increments.

In the RB model we choose the mass as $m_{\rm RB} = 0.01$ and in the RF model as $m_{\rm RF} = 0.02$. With these parameters, the probability ρ_0 to trigger a shock when moving $w \to w + 1$ is $\rho_0^{\rm RF} = (6.959 \pm 0.001) \times 10^{-3}$ and $\rho_0^{\rm RB} = (9.471 \pm 0.001) \times 10^{-3}$. These small values of the masses ensure that the models efficiently approximate our continuum model in $d = 0$, and that the particle optimizes its energy over a large number of random variables. We perform averages over 10 simulations of environments of size $N = 5 \times 10^8$ sites. We obtain excellent statistics for various observables studied in this work, including $\rho_2(W)$, $\Delta(W)$ measured using Eq. (23), $\langle S_1 S_2\rangle_{\rho_W}$ and $\langle S_1^2 S_2\rangle_{\rho_W}$.

Let us emphasize that these simulations are more a proof of principle to motivate simulations on higher dimensional models and measurements in experiments, than a full test of the results obtained in this article. This said, our simulations allow us to verify the exact result (40) to a very high accuracy. Second, although $d = 0$ is at a large value of ϵ in the $d = 4 - \epsilon$ expansion, the FRG equation and the associated fixed-point functions for random-field disorder are known to behave quite similarly [30, 43]. For random-bond disorder we expect less universality since $\Delta(u)$ is non-universal in $d = 0$; nevertheless the relations between the correlation and $\Delta(u)$ are interesting to investigate, in particular the sign of the correlations.

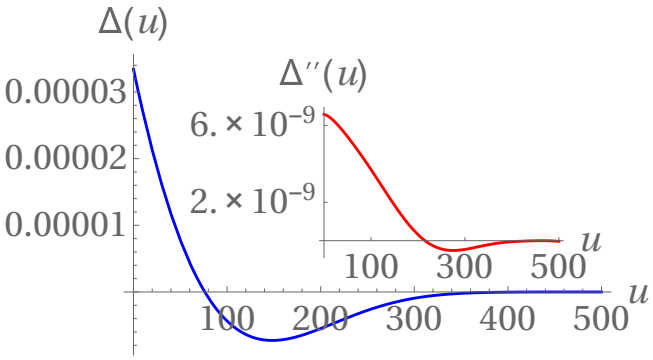

FIG. 2: Renormalized disorder $\Delta(u)$ measured in the $d = 0$ RB toy model. Inset: its second derivative $\Delta''(u)$, computed using a numerical fit of the measured $\Delta(u)$.

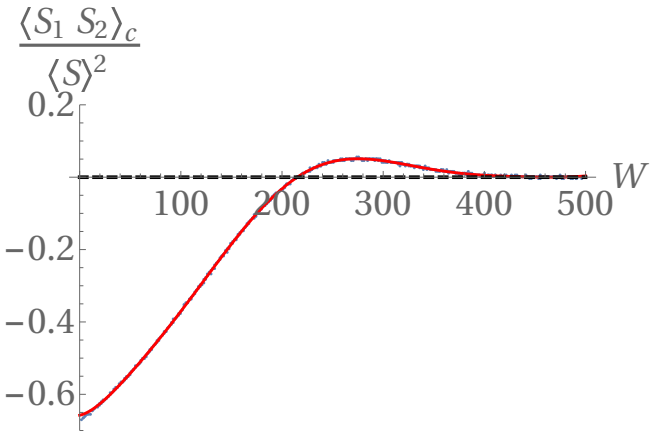

FIG. 3: Comparison between the measurement of the normalized moment $\frac{\langle S_1 S_2\rangle_{\rho^c_W}}{\langle S\rangle^2_\rho}$ (blue dots) and the prediction from the exact result (40) using the measurement of $\Delta(u)$ (red curve) in the RB toy model. The agreement is perfect as expected.

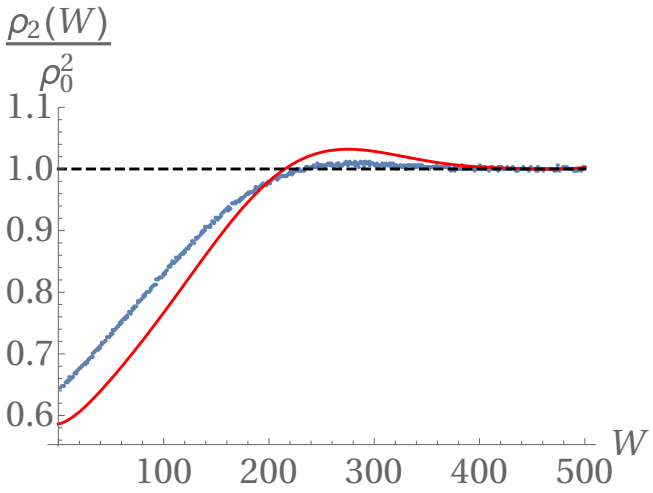

FIG. 4: Comparison between the measurement of $\rho_2(W)$ (blue dots) and the prediction from the $O(\epsilon)$ result (75) using the measurement of $\Delta(u)$ (red curve) in the RB toy model. We obtain a surprisingly good agreement.

B. Numerical Results: RB model

Using the definition (23) we measure the renormalized disorder correlator. The result is shown in Fig. 2. Using an interpolation of the result with a polynomial of degree 10, we obtain a smooth version that is later used to compute its second derivative $\Delta''(u)$ which appears in our analysis as the central object controlling the amplitude of the correlations. Some measured properties are: $\Delta(0) \approx 3.34 \times 10^{-5}$, $\Delta''(0) \approx 6.78 \times 10^{-9}$; $\Delta(76.2) \approx 0$, $\Delta''(215) \approx 0$; the position of the minimum and the value at the minimum: $\Delta(148.2) \approx -7.3 \times 10^{-6}$, $\Delta''(274,4) \approx -5.1 \times 10^{-10}$. This is compared with the measurement of $\langle S_1 S_2\rangle_{\rho_W}$ using the exact result (40), see Fig. 3. We obtain a perfect agreement.

From a qualitative perspective, we note the following:

(i) We observe the predicted crossover from anti-correlated shocks at small distances ($W < 215$) to positively correlated shocks at large distances.

(ii) The correlations are far from being negligible: by definition $\frac{\langle S_1 S_2\rangle_{\rho^c_W}}{\langle S\rangle_{\rho^2}} > -1$, while we observe $\frac{\langle S_1 S_2\rangle_{\rho^c_{W\approx 0}}}{\langle S\rangle^2_\rho} \approx -0.6$, an indication that the shocks in this toy model are strongly correlated.

We now check the predictions obtained using the ϵ expansion. We first measure $\rho_2(W)$ and compare it with the result (75), see Fig. 4. We obtain a surprisingly good agreement between the two curves, considering that $\epsilon = 4$. We also measure $\langle S_1^2 S_2\rangle_{\rho_W}$ and compare it with the result (67), see Fig. 5. Here the discrepancy is large for smaller values of W, a fact that can be anticipated since our result predicts $\frac{\langle S_1^2 S_2\rangle_{\rho^c_W}}{\langle S^2\rangle_\rho \langle S\rangle_\rho} < -1$ at small W, which is unphysical. This discrepancy keeps increasing with higher-order moments. However the sign of the correlation, and its value for large W is quite well predicted.

C. Numerical Results: RF model

In Figs. 6 to 9 we show the corresponding results for the RF toy model. They are similar except that as predicted in this type of model the shocks are *always anti-correlated*. The value at the origin of the renormalized disorder correlator and of its second derivative are measured as $\Delta(0) \approx 3.4 \times 10^{-3}$, $\Delta''(0) \approx 9.4 \times 10^{-8}$. Once again we observe that these correlations are large, $\frac{\langle S_1 S_2\rangle_{\rho^c_{W\approx 0}}}{\langle S\rangle^2_\rho} \approx -0.6$. We obtain a perfect agreement for the exact result $\langle S_1 S_2\rangle_{\rho_W}$, see Fig. 7. The agreement for the $O(\epsilon)$ result for $\rho_2(W)$ (75) is surprisingly good (see Fig. 8), whereas the $O(\epsilon)$ approximation breaks down for higher moments at small W such as $\langle S_1^2 S_2\rangle_{\rho^c_W}$, see Fig. 9.

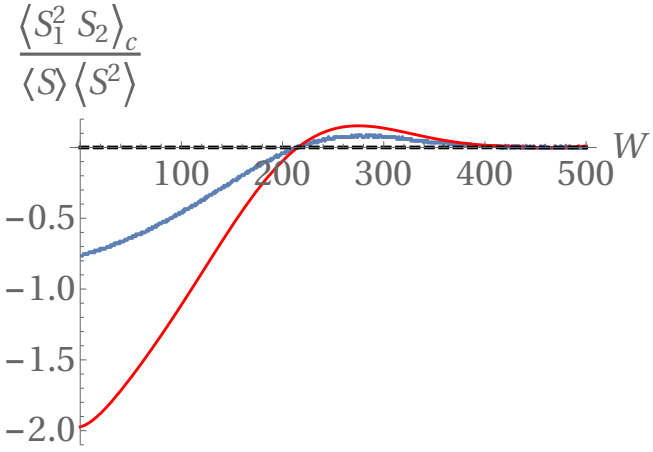

FIG. 5: Comparison between the measurement of the normalized moment $\frac{\langle S_1^2 S_2\rangle_{\rho^c_W}}{\langle S^2\rangle_\rho \langle S\rangle_\rho}$ (blue dots) and the prediction from the exact result (40) using the measurement of $\Delta(u)$ (red curve) in the RB toy model.

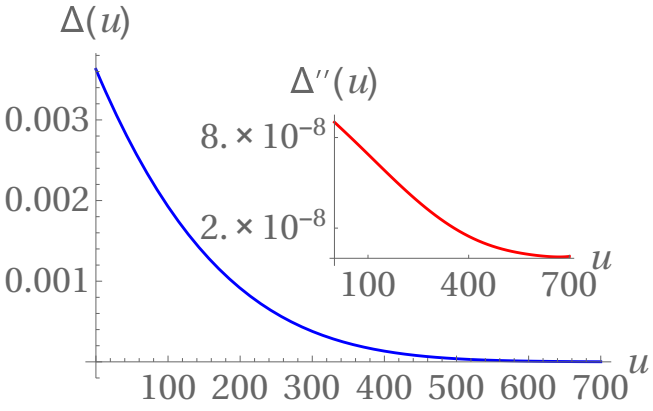

FIG. 6: Renormalized disorder $\Delta(u)$ measured in the $d = 0$ RF toy model. Inset: its second derivative $\Delta''(u)$, computed using a numerical fit of the measured $\Delta(u)$.

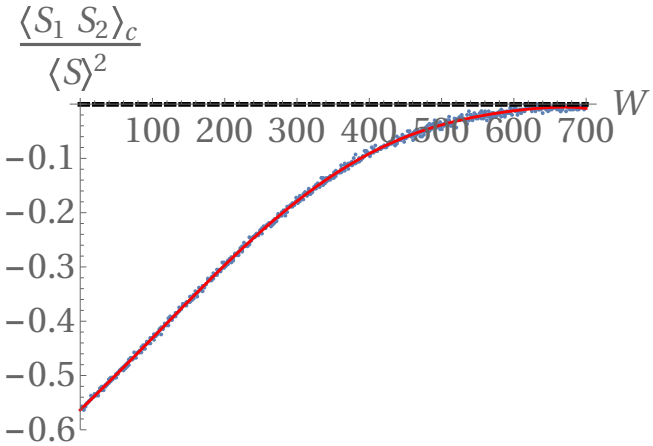

FIG. 7: Comparison between the measurement of the normalized moment $\frac{\langle S_1 S_2\rangle_{\rho^c_W}}{\langle S\rangle^2_\rho}$ (blue dots) and the prediction from the exact result (40) using the measurement of $\Delta(u)$ (red curve) in the RF toy model. The agreement is perfect as expected.

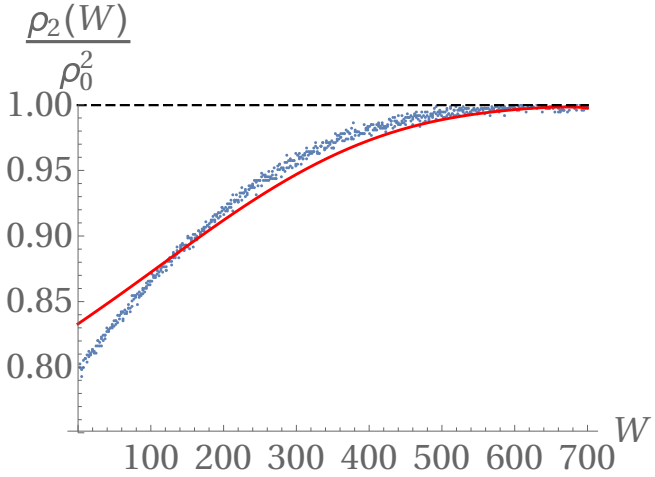

FIG. 8: Comparison between the measurement of $\rho_2(W)$ (blue dots) and the prediction from the $O(\epsilon)$ result (75) using the measurement of $\Delta(u)$ (red curve) in the RF toy model. The agreement is surprisingly good.

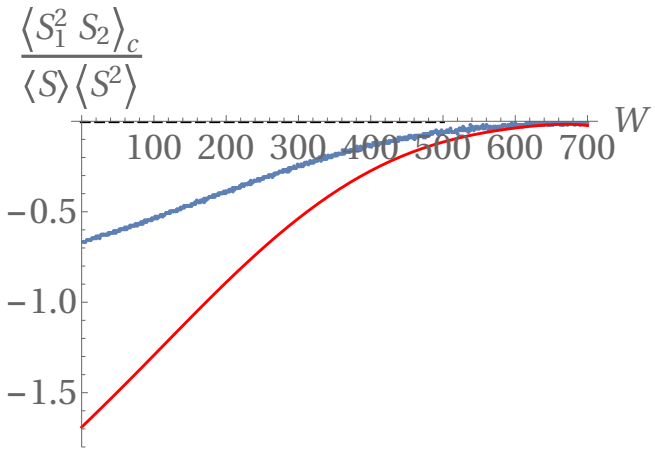

FIG. 9: Comparison between the measurement of the normalized moment $\frac{\langle S_1^2 S_2\rangle_{\rho^c_W}}{\langle S^2\rangle_\rho \langle S\rangle_\rho}$ (blue dots) and the prediction from the $O(\epsilon)$ result (40) using the measurement of $\Delta(u)$ (red curve) in the RF toy model.

VII. CONCLUSION

In this paper we shed light on the fact that, for realistic models of elastic interfaces in a random medium below their upper critical dimension, correlations between (static) avalanches should always be expected. To do so we have studied the correlations between the size and location of shocks in the ground state of elastic interfaces in a random potential. We found the exact relation (8) for the first connected moment that characterizes these correlations in terms of the renormalized disorder correlator, a universal quantity at the center of the FRG treatment of disordered elastic systems. Beyond the first cumulant, higher-order moments (70), (72) and the full joint density of shocks (74) were computed using the FRG at first

non-trivial order in the ϵ expansion. The local structure of these correlations was made precise through a study of local shock sizes. The qualitative phenomenology associated with these correlations clearly distinguishes between the Random-Bond and Random-Field universality classes. This was highlighted through a numerical simulation of $d = 0$ toy models.

We expect our results to broadly apply to models in the universality class of the statics of disordered elastic systems. Concerning the dynamics, and avalanches at the depinning transition of elastic interfaces, we expect our results to be equivalently *applicable and accurate*. The derivation of the exact relation (8) can easily be adapted to the dynamics by considering the quasi-static steady-state process of the position field of the interface instead of the position of its ground-state as was done in Ref. [33]. For the results at the improved tree level, it is expected that both theories are equivalent for those observables [33]. The most important difference is that in the dynamics the Random-Bond universality class is unstable, and thus the observed correlations should always be of the Random-Field type (at least as long as the microscopic disorder is short-ranged).

For physical systems where the usual model of elastic interfaces is accurate, our results give a precise description of the correlations. Even if additional mechanisms generating correlations are present, such as in earthquake problems, correlations due to the short-ranged nature of the disorder as described in this work should be included in order to gain a quantitative understanding of the correlations due to these additional mechanisms.

Acknowledgments

We warmly thank Alexander Dobrinevski for numerous discussions. We acknowledge hospitality from the KITP in Santa Barbara where part of this work was conducted. This research was supported in part by the National Science Foundation under Grant No. NSF PHY11-25915. We acknowledge support from PSL grant ANR-10-IDEX-0001-02-PSL.

Appendix A: Proof of the identity on generating functions

As in the case of one shock (Appendix A of [31]), the important identity is

$$(\partial_\delta + \lambda L^d) e^{\lambda L^d (u(w+\delta)-w-\delta)} = \sum_i (e^{\lambda S_i} - 1) e^{\lambda L^d [u(w_i^-)-w-\delta]} \delta(w + \delta - w_i) \tag{A1}$$

By definition $u(w_i^-) = L^{-d} \sum_{j<i} S_j$. Let us consider

$$\begin{aligned} G_{w_1,w_2}(\delta_1,\delta_2) &= (\partial_{\delta_1} + \lambda_1 L^d)(\partial_{\delta_2} + \lambda_2 L^d) \times \\ & e^{\lambda_1 L^d [u(w_1+\delta_1)-u(w_1)-\delta_1] + \lambda_2 L^d [u(w_2+\delta_2)-u(w_2)-\delta_2]} \\ &= \sum_{ij} (e^{\lambda_1 S_i} - 1)(e^{\lambda_2 S_j} - 1) e^{\lambda_1 L^d [u(w_i^-)-u(w_1)-\delta_1]} \times \\ & e^{\lambda_2 L^d [u(w_j^-)-u(w_2)-\delta_2]} \delta(w_1 + \delta_1 - w_i) \delta(w_2 + \delta_2 - w_j) \end{aligned} \tag{A2}$$

Taking advantage of the Dirac δ-function, we can replace the $u(w_1)$ inside the exponential by $u(w_i - \delta_1)$ which unambiguously gives $u(w_i^-)$ when one takes the limit of $\delta_1 \to 0^+$. We thus obtain

$$\lim_{\delta_1,\delta_2 \to 0^+} G_{w_1,w_2}(\delta_1,\delta_2) = \sum_{ij} (e^{\lambda_1 S_i} - 1)(e^{\lambda_2 S_j} - 1) \delta(w_1 - w_i) \delta(w_2 - w_j). \tag{A3}$$

Taking the average over disorder, we obtain by definition of $Z_{w_2-w_1}(\lambda_1, \lambda_2)$

$$Z_{w_2-w_1}(\lambda_1,\lambda_2) = \lim_{\delta_1,\delta_2 \to 0^+} L^{-2d} \overline{G_{w_1,w_2}(\delta_1,\delta_2)}\,. \tag{A4}$$

On the other hand, developing $(\partial_{\delta_1} + \lambda_1 L^d)(\partial_{\delta_2} + \lambda_2 L^d) = \partial_{\delta_1}\partial_{\delta_2} + L^d \lambda_1 \partial_{\delta_2} + L^d \lambda_2 \partial_{\delta_1} + L^{2d} \lambda_1 \lambda_2$ in the expression of $G_{w_1,w_2}(\delta_1,\delta_2)$ one arrives at Eqs. (46) and (47).

Appendix B: Diagrammatic rules for two-shocks moments

In this appendix we explain the rules (i), (ii) and (iii) that were stated and used in Sec. IV to obtain diagrammatically the result (70).

These rules come from the fact that in the $\mathcal{K}$ operation each external leg produces an additional factor of δ_1 (for the n legs at $w_1, \dots w_n \approx 0$) or δ_2 (for the m legs at $w_{n+1}, \dots w_{n+m} \approx W$), thus tend to be of higher order in δ_1 and δ_2. However, from the study of the one-shock case (see Section V.C of [31]), we know the general mechanism to escape this apparent trivialization and to allow that each part of the diagram that connects only coinciding points together brings a single δ_i. In this case, starting from the top of a diagram the δ_i attached to an external leg can be brought to the bottom of the diagram as long as the disorder vertex encountered along the way leads to a $\Delta'(0^+)$ when taking the limit of coinciding points. In such diagrams each vertex linking coinciding points must have two up-going propagators and one entering from below (effectively corresponding to the $\Delta'(0^+)$ cubic vertex of the BFM [33]), except for the vertex at the bottom of the diagram which has only two up-going propagators (see Section V.D. of [31]). This last vertex is the one carrying the remaining factor of δ_1: being differentiated in the end it also leads to an additional factor of $\Delta'(0^+)$.

This explains why the disorder only enters as $\Delta'(0^+)$ in the one-shock improved-tree-theory result (58). The rule (iii) stated above is a generalization of that property.

In the two-shock case the same mechanism occurs and rule (i) is obvious: a diagram cannot have more than two sets of points separated by a double-dashed line (one around $w \approx 0$ and one around $w \approx W$) since each set contributes a factor of δ_i. For example, in the last diagram of Eq. (66), each leg is such a set of points, and the diagram is $O(\delta_1^2\delta_2)$. To explain rule (ii), let us consider one endpoint of a double-dashed line and distinguish three cases. First, if there is no propagator entering from below this point, such as the points at $w \approx W$ in the first and second diagrams of Eq. (66) and the two points in Eq. (63), then the δ_i originating from the set of connected points above it end at this vertex, and the vertex is differentiated during the $\mathcal{K}$ operation. Second, if there is a propagator entering from below that point, such as the point at $w_1 \approx 0$ in the first diagram of Eq. (66), then the δ_i originating from above the vertex continues downward the diagram without modifying the vertex. Third, if there is more than one propagator entering from below the point then the diagram will necessarily be of higher order in δ_i. Combining these three cases, one concludes that the double-dashed-line vertex necessarily corresponds to a $\Delta''(W)$.

Appendix C: A derivation from the Carraro-Duchon formula

Let us recall the results obtained in Ref. [32], generalizing to arbitrary dimension the result from Ref. [42]. Consider

$$e^{L^d\hat{\mathbb{Z}}_t\{\omega_i,w_i\}} := \overline{e^{\frac{-L^d}{t}\sum_{i=1}^p \omega_i[u(w_i)-w_i]}} \ , \qquad \text{(C1)}$$

where $t := \frac{1}{m^2}$. Then, in the improved-tree theory, $\hat{\mathbb{Z}}$ solves the differential equation

$$\partial_t\hat{\mathbb{Z}}_t\{\omega_i,w_i\} = -\sum_{i=1}^p \frac{\partial}{\partial\omega_i}\hat{\mathbb{Z}}_t\{\omega_i,w_i\}\frac{\partial}{\partial w_i}\hat{\mathbb{Z}}_t\{\omega_i,w_i\}$$
$$\hat{\mathbb{Z}}_{t=0}\{\omega_i,w_i\} = \frac{1}{2}\sum_{i,j=1}^p \omega_i\omega_j\Delta(w_i-w_j) \ . \qquad \text{(C2)}$$

It further satisfies the STS symmetry relation,

$$\hat{\mathbb{Z}}_t\{\omega_i,w_i+\delta w\} = \hat{\mathbb{Z}}_t\{\omega_i,w_i\}$$
$$\sum_i \frac{\partial}{\partial w_i}\hat{\mathbb{Z}}_t\{\omega_i,w_i\} = 0 \ . \qquad \text{(C3)}$$

In order to extract the needed information for the two-shock statistics we choose $p = 4$ and the quadruplets $(\omega_1,\omega_2,\omega_3,\omega_4) = (-\omega_1-\tilde{\omega},\omega_1,-\omega_2+\tilde{\omega},\omega_2)$ and $(w_1,w_2,w_3,w_4) = (0,\delta_1,W,W+\delta_2)$. We then consider (with a slight abuse of notations)

$$\tilde{\mathbb{Z}}_t(\omega_1,\delta_1,\tilde{\omega},W,\omega_2,\delta_2) \qquad \text{(C4)}$$
$$= \hat{\mathbb{Z}}_t(-\omega_1-\tilde{\omega},0,\omega_1,\delta_1,-\omega_2+\tilde{\omega},W,\omega_2,W+\delta_2)$$

Because of the STS the $p = 4$ function $\tilde{\mathbb{Z}}_t$ depends only on six variables (and not eight) and satisfies a closed equation. Indeed, using Eqs. (C2) and (C3), one proves that $\tilde{\mathbb{Z}}_t$ satisfies the following evolution equation

$$\partial_t\tilde{\mathbb{Z}}_t = -\left(\frac{\partial}{\partial\omega_1}\tilde{\mathbb{Z}}_t\frac{\partial}{\partial\delta_1}\tilde{\mathbb{Z}}_t + \frac{\partial}{\partial\tilde{\omega}}\tilde{\mathbb{Z}}_t\frac{\partial}{\partial W}\tilde{\mathbb{Z}}_t + \frac{\partial}{\partial\omega_2}\tilde{\mathbb{Z}}_t\frac{\partial}{\partial\delta_2}\tilde{\mathbb{Z}}_t\right) \qquad \text{(C5)}$$

We are only interested in a perturbative resolution. Define the expansion

$$\tilde{\mathbb{Z}}_t = \sum_{mnp} z^p_{mn}(t,\omega_1,\omega_2,W)\delta_1^m\delta_2^n\tilde{w}^p \ . \qquad \text{(C6)}$$

Indeed, this is sufficient to retrieve the generating function $\hat{Z}_W(\lambda_1,\lambda_2) = \hat{Z}^{\rm disc}_W(\lambda_1,\lambda_2) + \hat{Z}^c_W(\lambda_1,\lambda_2)$ as (compare with the small-δ_i expansion of (C1) and (47))

$$\hat{Z}^{\rm disc}_W(\lambda_1,\lambda_2) = z^0_{10}(\omega_1,\omega_2,W)z^0_{01}(\omega_1,\omega_2,W)$$
$$\hat{Z}^c_W(\lambda_1,\lambda_2) = L^{-d}z^0_{11}(\omega_1,\omega_2,W) \ . \qquad \text{(C7)}$$

On the right-hand side the arguments are $\omega_1 = -t\lambda_1$ and $\omega_2 = -t\lambda_2$. Inserting the expansion (C6) inside Eq. (C5), we obtain the initial conditions:

$$\begin{aligned}
z^0_{00}(t=0,\omega_1,\omega_2,W) &= 0\\
z^0_{10}(t=0,\omega_1,\omega_2,W) &= -\Delta'(0^+)\omega_1^2\\
z^0_{01}(t=0,\omega_1,\omega_2,W) &= -\Delta'(0^+)\omega_2^2\\
z^0_{11}(t=0,\omega_1,\omega_2,W) &= -\Delta''(W)\omega_1\omega_2\\
z^1_{00}(t=0,\omega_1,\omega_2,W) &= 0 \ .
\end{aligned} \qquad \text{(C8)}$$

Obviously we have $z^0_{00}(t,\omega_1,\omega_2,W) = 0$, $\forall t$. We also obtain the evolution equation:

$$\begin{aligned}
\partial_t z^0_{10} &= -\Big(\frac{\partial}{\partial\omega_1}z^0_{10}\Big)z^0_{10} - \Big(\frac{\partial}{\partial\omega_2}z^0_{10}\Big)z^0_{01} - z^1_{00}\frac{\partial}{\partial W}z^0_{10}\\
\partial_t z^0_{01} &= -\Big(\frac{\partial}{\partial\omega_1}z^0_{01}\Big)z^0_{10} - \Big(\frac{\partial}{\partial\omega_2}z^0_{01}\Big)z^0_{01} - z^1_{00}\frac{\partial}{\partial W}z^0_{01}\\
\partial_t z^0_{11} &= -\Big(\frac{\partial}{\partial\omega_1}z^0_{10}\Big)z^0_{11} - \Big(\frac{\partial}{\partial\omega_1}z^0_{01}\Big)2z^0_{20} - \Big(\frac{\partial}{\partial\omega_1}z^0_{11}\Big)z^0_{10}\\
&\quad -\Big(\frac{\partial}{\partial\omega_2}z^0_{10}\Big)2z^0_{02} - \Big(\frac{\partial}{\partial\omega_2}z^0_{01}\Big)z^0_{11} - \Big(\frac{\partial}{\partial\omega_2}z^0_{11}\Big)z^0_{01}\\
&\quad -z^1_{00}\frac{\partial}{\partial W}z^0_{11} - z^1_{10}\frac{\partial}{\partial W}z^0_{01} - z^1_{01}\frac{\partial}{\partial W}z^0_{10}\\
\partial_t z^1_{00} &= -\Big(\frac{\partial}{\partial\omega_1}z^1_{00}\Big)z^0_{10} - \Big(\frac{\partial}{\partial\omega_2}z^1_{00}\Big)z^0_{01} - z^1_{00}\frac{\partial}{\partial W}z^1_{00}
\end{aligned} \qquad \text{(C9)}$$

As a consequence of the initial conditions (C8), one can look for a solution of Eq. (C9) such that

$$\frac{\partial}{\partial\omega_2}z^0_{10} = \frac{\partial}{\partial\omega_1}z^0_{01} = \frac{\partial}{\partial W}z^0_{10} = \frac{\partial}{\partial W}z^0_{01} = z^1_{00} = 0 \ . \qquad \text{(C10)}$$

Each term has an interpretation in the notations of the main text. z^0_{10} corresponds to $\hat{Z}(\lambda_1)$ and z^0_{01} corresponds to $\hat{Z}(\lambda_2)$, which in the present notations reads

(see Eqs. (43) and (58) and recall $S_m = \sigma/m^4 = \sigma t^2$)

$$z^0_{10}(\omega_i) = \hat{Z}(\lambda_i) = \frac{1 + 2\sigma\omega_i t - \sqrt{1+4\sigma\omega_i t}}{2\sigma t^2} \ . \quad \text{(C11)}$$

This is the solution of Eq. (C9) using Eq. (C10). Note that $z^1_{00} = 0$ can be seen as the signature that diagrams contributing to the avalanche at $w = 0$ and at $w = W$ can be linked only by one vertex $\Delta''(W)$, as observed in the diagrammatics, see Eq. (69). This is already present in the initial condition (C8). The equation for z^0_{11} becomes

$$\begin{aligned} \partial_t z^0_{11} \ &= \ -\Big(\frac{\partial}{\partial\omega_1} z^0_{10}\Big) z^0_{11} - \Big(\frac{\partial}{\partial\omega_1} z^0_{11}\Big) z^0_{10} \\ &\quad -\Big(\frac{\partial}{\partial\omega_2} z^0_{01}\Big) z^0_{11} - \Big(\frac{\partial}{\partial\omega_2} z^0_{11}\Big) z^0_{01} \ . \end{aligned} \quad \text{(C12)}$$

One can check that the result (70) obtained diagrammatically in the main text, and which in the present notations reads

$$z^0_{11} = -\frac{\Delta''(W)}{4\sigma^2 t^2} \frac{1-\sqrt{1+4\sigma\omega_1 t}}{\sqrt{1+4\sigma\omega_1 t}} \frac{1-\sqrt{1+4\sigma\omega_2 t}}{\sqrt{1+4\sigma\omega_2 t}} \ ,$$

solves this equation with the initial condition (C8). This demonstrates the equivalence of the two methods and results.

Appendix D: Saddle-point calculation for the local structure.

1. Algebraic derivation of Eq. (107)

In this appendix we prove formula (107) "from first principles" using a saddle-point calculation on the improved action (57). This computation is similar to the one presented in Ref. [32] for the calculation of the one-shock density. Here the observable of interest is

$$\begin{aligned} &\hat{Z}^{\phi^1\phi^2}_W(\lambda_1,\lambda_2) = \frac{1}{\int_x \phi^1_x \int_x \phi^2_x} \lim_{\delta_1,\delta_2\to 0^+} \partial_{\delta_1,\delta_2} G_W(\delta_1,\delta_2) \\ &G_W(\delta_1,\delta_2) = \\ &\qquad \overline{e^{\int_x \phi^1_x \lambda_1 (\hat{u}_x(w_1+\delta_1) - \hat{u}_x(w_1))} e^{\int_x \phi^2_x \lambda_2 (\hat{u}_x(w_2+\delta_2) - \hat{u}_x(w_2))}}, \end{aligned} \quad \text{(D1)}$$

where $w_2 = w_1 + W$. This observable can be expressed using the improved action $\Gamma[u]$ of the replicated field theory (57) with $i = 1,\dots,4$ sets of $a = 1,\dots,n$ replicated position fields $\tilde{u}^i_{ax}$ feeling a parabolic well at position $\tilde{w}_i$ with $\tilde{w}_1 = w_1$, $\tilde{w}_2 = w_1 + \delta_1$, $\tilde{w}_3 = w_1 + W$, $\tilde{w}_4 = w_1 + W + \delta_2$:

$$G_W(\delta_1,\delta_2) = \int \mathcal{D}[u] e^{\int_x \sum_{i=1}^4 \nu_i \psi^i_x (u^i_{1x} - \tilde{w}_i) - \Gamma[u]} \quad \text{(D2)}$$

Here and for the rest of this appendix, the $n \to 0$ limit is implicit. To compute the disorder average we have singled out replica $a = 1$. In order to write the formulas in a compact form, we introduced new variables $\nu_2 = \lambda_1$, $\nu_1 = -\lambda_1$, $\nu_4 = \lambda_2$, $\nu_3 = -\lambda_2$, $\psi^1_x = \psi^2_x = \phi^1_x$, $\psi^3_x = \psi^4_x = \phi^2_x$. At the improved tree level, the functional integral is evaluated through a saddle-point calculation as

$$G_W(\delta_1,\delta_2) = e^{\int_x \sum_{i=1}^4 \nu_i \psi^i_x (u^i_{1x} - \tilde{w}_i) - \Gamma[u]} \ , \quad \text{(D3)}$$

where the position fields u^i_{ax} solve the saddle-point equation

$$\int_{x'} g^{-1}_{xx'}(u^i_{ax'} - \tilde{w}_i) - \frac{1}{T}\sum_{cj} R'(u^i_{ax} - u^j_{cx}) = T\nu_i \psi^i_x \delta_{a1} \ . \quad \text{(D4)}$$

We are interested in the solution of Eq. (D4) in the $T \to 0$ limit. As in Ref. [32], we look for a solution that isolates the first replica ($a = 1$) in each set ($i = 1,\dots,4$) of position fields as

$$u^i_{ax} = u^i_x - (1-\delta_{a1}) T U^i_x. \quad \text{(D5)}$$

Inserting the Ansatz (D5) into (D4) leads to

$$\begin{aligned} &\int_{x'} g^{-1}_{xx'}(u^i_{1x'} - \tilde{w}_i) + \sum_j R''(u^i_{1x} - u^j_{1x}) U^j_x = 0 \\ &\int_{x'} g^{-1}_{xx'} U^i_{x'} + \sum_{j\neq i} R'''(u^i_{1x} - u^j_{1x}) U^i_x U^j_x = \nu_i \psi^i_x \ . \end{aligned}$$

Being ultimately interested in the computation of (D1), we solve this equation in an expansion in δ_1 and δ_2 as

$$\begin{aligned} u^1_x &= \frac{\tilde{w}_1 + \tilde{w}_2}{2} - u^{11}_x \delta_1 + u^{12}_x \delta_2 \\ u^2_x &= \frac{\tilde{w}_1 + \tilde{w}_2}{2} + u^{21}_x \delta_1 + u^{22}_x \delta_2 \\ u^3_x &= \frac{\tilde{w}_3 + \tilde{w}_4}{2} + u^{31}_x \delta_1 - u^{32}_x \delta_2 \\ u^4_x &= \frac{\tilde{w}_3 + \tilde{w}_4}{2} + u^{41}_x \delta_1 + u^{42}_x \delta_2 \\ U^i_x &= U^{i0}_x + U^{i1}_x \delta_1 + U^{i2}_x \delta_2. \end{aligned} \quad \text{(D6)}$$

Using now the definition (D1) we need to perform the following derivatives of (D3), $\partial_{\delta_1}\partial_{\delta_2} = \partial_{\tilde{w}_2}\partial_{\tilde{w}_4}$. Since the fields u^i_{ax} are evaluated at the saddle point, we can differentiate only with respect to the explicit dependence in the $\tilde{w}_i$. Using the form (57) for $\Gamma[u]$, these derivatives can be calculated by repeating the identity

$$\partial_{\tilde{w}_i} G_W = \left(-\nu_i \int_x \psi^i_x + \frac{1}{T}\sum_{ai} \int_{xx'} g^{-1}_{xx'}(u^i_{ax'} - \tilde{w}_i) \right) G_W \ .$$

Using that $\lim_{n\to 0} \sum_a (u^i_{ax} - \tilde{w}_i) = T U^i_x$ we obtain the following decomposition

$$\hat{Z}^{\phi^1\phi^2}_W(\lambda_1,\lambda_2) = \hat{Z}^{\phi^1}(\lambda_1)\hat{Z}^{\phi^2}(\lambda_2) + \hat{Z}^{c,\phi^1\phi^2}_W(\lambda_1,\lambda_2) \quad \text{(D7)}$$

with the explicit forms

$$\begin{aligned} \hat{Z}^{\phi^1}(\lambda_1) &= \frac{\int_x (-\nu_2 \psi^2_x + \int_{x'} g^{-1}_{xx'} U^{20}_{x'})}{\int_x \psi^2_x} \\ \hat{Z}^{\phi^2}(\lambda_2) &= \frac{\int_x (-\nu_4 \psi^4_x + \int_{x'} g^{-1}_{xx'} U^{40}_{x'})}{\int_x \psi^4_x} \end{aligned} \quad \text{(D8)}$$

and

$$\hat{Z}_W^{c,\phi^1\phi^2}(\lambda_1,\lambda_2) = \frac{1}{\int\psi_x^2\int\psi_x^4}\int_x\int_{x'} g^{-1}_{xx'}U^{22}_{x'} = \frac{1}{\int\psi_x^2\int\psi_x^4}\int_x\int_{x'} g^{-1}_{xx'}U^{41}_{x'} \ . \quad \text{(D9)}$$

Although not obvious, these definitions are in agreement with those of the main text. Despite their complexity, the equations satisfied by the u and U variables obey several symmetries. The important ones are $U^{10}_x = -U^{20}_x$ and $U^{30}_x = -U^{40}_x$; $U^{11}_x = -U^{21}_x$ and $U^{32}_x = -U^{42}_x$; $U^{12}_x = -U^{22}_x$ and $U^{31}_x = -U^{41}_x$; $u^{11}_x = u^{21}_x$ and $u^{32}_x = u^{42}_x$; $u^{12}_x = u^{22}_x$ and $u^{31}_x = u^{41}_x$. We also have $U^{22}_x = U^{41}_x$.

Using these symmetries, one finds that U^{20}_x and U^{40}_x satisfy

$$\int_{x'} g^{-1}_{xx'}U^{20}_{x'} = \sigma(U^{20}_x)^2 + \nu_2\psi_x^2 \ ,$$
$$\int_{x'} g^{-1}_{xx'}U^{40}_{x'} = \sigma(U^{40}_x)^2 + \nu_4\psi_x^4 \ , \quad \text{(D10)}$$

where $\sigma = R'''(0^+)$. Note that these are related to the function $Z^\phi_x(\lambda)$ defined in the main text in Eq. (96) through the relation $Z^{\phi^1}_x(\lambda_1) = \int_{x'} g^{-1}_{xx'}U^{20}_{x'}$. Hence, Eq. (D8) leading to the disconnected part of the result for $\hat{Z}_W^{\phi^1\phi^2}(\lambda_1,\lambda_2)$ is in agreement with the main text. Let us now introduce two important kernels defined as the functional derivatives $K_2(x,z) = \frac{\delta U^{20}_x}{\nu_2\delta\psi^2_z}$ and $K_4(x,z) = \frac{\delta U^{40}_x}{\nu_4\delta\psi^4_z}$. They satisfy

$$\int_{x'} g^{-1}_{xx'}K_2(x',z) - 2\sigma U^{20}_x K_2(x,z) = \delta(x-z)$$
$$\int_{x'} g^{-1}_{xx'}K_4(x',z) - 2\sigma U^{40}_x K_4(x,z) = \delta(x-z)$$

and are important building blocks in our calculation. These kernels are symmetric: the kernel of the operator K_2^{-1} is given by $K_2^{-1}(x,x') = g^{-1}_{xx'} - 2\sigma U_{20x}\delta(x-x')$. In particular it is a symmetric function of its arguments, and thus $K_2(x,z)$ also is a symmetric function. The analytic expressions of the functions U^{20}_x and U^{40}_x are hard to obtain in generality. In Ref. [31] they were obtained for avalanches measured on hyperplanes for SR elasticity: $\psi^2_x = \delta(x_1)$ where x_1 denotes the first coordinate of the d-dimensional variable x. We recall this explicit solution below in Appendix D 2.

a. Solutions for the u variables

Let us first consider the solution for the u variables. The equations read

$$\int_{x'} g^{-1}_{xx'}\Big(\frac{1}{2} - u^{11}_{x'}\Big) - 2\sigma U^{10}_x u^{11}_x = 0$$
$$\int_{x'} g^{-1}_{xx'}u^{31}_{x'} = 2u^{11}_x U^{10}_x R'''(W)$$
$$\int_{x'} g^{-1}_{xx'}\Big(\frac{1}{2} - u^{32}_{x'}\Big) - 2\sigma U^{30}_x u^{32}_x = 0$$
$$\int_{x'} g^{-1}_{xx'}u^{12}_{x'} = 2u^{32}_x U^{30}_x R'''(W) \quad \text{(D11)}$$

The solutions are expressed in terms of the two kernels as

$$u^{11}_x = u^{21}_x = -\frac{\sigma}{R'''(W)}u^{31}_x + \frac{1}{2} = -\frac{\sigma}{R'''(W)}u^{41}_x + \frac{1}{2} = \frac{m^2}{2}\int_z K_2(x,z) \quad \text{(D12)}$$
$$u^{32}_x = u^{42}_x = -\frac{\sigma}{R'''(W)}u^{12}_x + \frac{1}{2} = -\frac{\sigma}{R'''(W)}u^{22}_x + \frac{1}{2} = \frac{m^2}{2}\int_z K_4(x,z) \quad \text{(D13)}$$

b. Solutions for the U variables

For the U variables, the equations read

$$\int_{x'} g^{-1}_{xx'}U^{21}_{x'} - 2\sigma U^{20}_x U^{21}_x - 2R^{(4)}(0)u^{11}_x(U^{20}_x)^2 = 0$$
$$\int_{x'} g^{-1}_{xx'}U^{42}_{x'} - 2\sigma U^{40}_x U^{42}_x - 2R^{(4)}(0)u^{32}_x(U^{40}_x)^2 = 0$$
$$\int_{x'} g^{-1}_{xx'}U^{22}_{x'} - 2\sigma U^{20}_x U^{22}_x - 2R^{(4)}(W)u^{32}_x U^{20}_x U^{40}_x = 0$$
$$\int_{x'} g^{-1}_{xx'}U^{41}_{x'} - 2\sigma U^{40}_x U^{41}_x - 2R^{(4)}(W)u^{11}_x U^{40}_x U^{20}_x = 0 \quad \text{(D14)}$$

Its solutions are

$$U^{11}_x = -U^{21}_x = -2R^{(4)}(0)\int_z K_2(x,z)u^{11}_z(U^{20}_z)^2$$
$$U^{32}_x = -U^{42}_x = -2R^{(4)}(0)\int_z K_2(x,z)u^{32}_z(U^{40}_z)^2$$
$$U^{12}_x = -U^{22}_x = -2R^{(4)}(W)\int_z K_2(x,z)u^{32}_z U^{20}_z U^{40}_z$$
$$U^{31}_x = -U^{41}_x = -2R^{(4)}(W)\int_z K_4(x,z)u^{11}_z U^{20}_z U^{40}_z \quad \text{(D15)}$$

c. Final result

Using Eq. (D9) we obtain

$$\hat{Z}_W^{c;\phi_1,\phi_2}(\lambda_1,\lambda_2) = \frac{1}{\int \psi_x^2 \int \psi_x^4} R^{(4)}(W) m^4 \int_{x',z,z'} K_2(x',z) U_z^{20} U_z^{40} K_4(z',z) \tag{D16}$$

Using the above results $U_x^{20} = \int_{x'} g_{xx'} Z_{x'}^{\phi_1}(\lambda_1)$, and $U_x^{40} = \int_{x'} g_{xx'} Z_{x'}^{\phi_2}(\lambda_2)$, as well as $K_2(x,z) = \int_{x'} g_{xx'} \frac{\delta Z_{x'}^{\phi^1}(\lambda_1)}{\lambda_1 \delta \phi_z^1}$ and $K_4(x,z) = \int_{x'} g_{xx'} \frac{\delta Z_{x'}^{\phi^2}(\lambda_2)}{\lambda_2 \delta \phi_z^2}$; remembering that $\psi_x^2 = \phi_x^1$ and $\psi_x^4 = \phi_x^2$, one shows that this formula is equivalent to Eq. (107).

d. Simplified form of the final result

The equivalent results (D16) and (107) both involve a functional derivative, which is in general a rather complicated object. We can however obtain a simplified formulation. From Eq. (D16) it is clear that it is sufficient to compute, for $i = 1, 2$,

$$\chi_i(x) = \int_z K_i(z,x) = \int_z K_i(x,z) \tag{D17}$$

rather than the full kernel K_i, and using the symmetry of K_i. Integrating Eq. (D11) over z one shows that $\chi_i(x)$ solves the equation

$$\int_{x'} g_{xx'}^{-1} \chi_2(x') - 2\sigma U_x^{20} \chi_2(x) = 1 \ ,$$
$$\int_{x'} g_{xx'}^{-1} \chi_4(x') - 2\sigma U_x^{40} \chi_4(x) = 1 \ .$$

Solving these equations (a task a priori simpler than the computation of the functional derivative) then leads to, following (D16),

$$\hat{Z}_W^{c;\phi_1,\phi_2}(\lambda_1,\lambda_2) = -\frac{1}{\int \phi_x^1 \int \phi_x^2} \Delta''(W) m^4 \int_z \chi_2(z) U_z^{20} U_z^{40} \chi_4(z) \ . \tag{D18}$$

2. More explicit solution for avalanches measured on parallel hyperplanes

a. Setting

We now obtain more explicit formulas in the case where avalanches are measured on two parallel hyperplanes at a distance $y > 0$ from one another and where the elasticity is short-ranged with kernel (15). That is, noting for definiteness x_1 the first coordinate of the d-dimensional vector x,

$$\phi_x^1 = \delta(x_1) \quad , \quad \phi_x^2 = \delta(x_1 - y) \ . \tag{D19}$$

In this case the problem becomes effectively unidimensional and the functions U and χ entering into Eq. (D18) only depend on x_1, abbreviated as x in the following. Furthermore, by translational invariance we can write

$$\begin{aligned} U_x^{20} &= Y(\lambda_1, x) \quad , \quad \chi_2(x) = \chi(\lambda_1, x) \\ U_x^{40} &= Y(\lambda_2, x-y) \quad , \quad \chi_4(x) = \chi(\lambda_2, x-y) \ . \end{aligned} \tag{D20}$$

These quantities obey the equations

$$\left(-\frac{d^2}{dx^2} + m^2\right) Y(\lambda, x) - \sigma \left(Y(\lambda, x)\right)^2 = \lambda \delta(x) \tag{D21}$$
$$\left(-\frac{d^2}{dx^2} + m^2\right) \chi(\lambda, x) - 2\sigma Y(\lambda, x) \chi(\lambda, x) = 1.$$

Solving these equations then leads to

$$\hat{Z}_W^{c;\phi_1,\phi_2}(\lambda_1,\lambda_2) = \frac{1}{L^{d-1}} R^{(4)}(W) m^4 \times \times \int_x \chi(\lambda_1, x) Y(\lambda_1, x) Y(\lambda_2, x-y) \chi(\lambda_2, x-y) \ . \tag{D22}$$

b. Solution for Y

The solution $Y(\lambda, x)$ of equation (D21) is already known in the literature, see Ref. [34] for details. It admits a scaling form

$$Y(\lambda, x) = \frac{m^2}{\sigma} \tilde{Y}\Big(\frac{\sigma}{m^3}\lambda, mx\Big) \ , \tag{D23}$$

where $\tilde{Y}(\tilde{\lambda}, \tilde{x})$ solves

$$\left(-\frac{d^2}{d\tilde{x}^2} + 1\right) \tilde{Y}(\tilde{\lambda}, \tilde{x}) - \Big(\tilde{Y}(\tilde{\lambda}, \tilde{x})\Big)^2 = \tilde{\lambda} \delta(\tilde{x}) \ . \tag{D24}$$

An explicit solution is

$$\tilde{Y}(\tilde{\lambda}, \tilde{x}) = \frac{6(1-z^2)e^{-|\tilde{x}|}}{\left(1 + z + (1-z)e^{-|\tilde{x}|}\right)^2} \ , \tag{D25}$$

where $z(\tilde{\lambda})$ is one of the solutions of

$$\tilde{\lambda} = 3z(1-z^2) \ . \tag{D26}$$

The right solution is uniquely defined from the following properties: it is defined for $\tilde{\lambda} \in]-\infty, \tilde{\lambda}_c = 2/\sqrt{3}[$, decreases from $z(-\infty) = \infty$ to $z_c = z(\tilde{\lambda}_c) = 1/\sqrt{3}$ and approaches 1 as $\tilde{\lambda}$ approaches 0.

c. Solution for χ

From the coupled equations (D21), it is seen that $\chi(\lambda, x)$ can be deduced from $Y(\lambda, x)$ as

$$\chi(\lambda, x) = \frac{1}{m^2} - \frac{2\sigma}{m^2} \frac{\partial Y}{\partial m^2} \ . \tag{D27}$$

Using the scaling form (D23) we obtain

$$\chi(\lambda,x)=\frac{1}{m^2}\tilde{\chi}\left(\tilde{\lambda}=\lambda\frac{\sigma}{m^3},\tilde{x}=mx\right)\ , \tag{D28}$$

where

$$\tilde{\chi}=1-2\tilde{Y}+3\tilde{\lambda}\partial_{\tilde{\lambda}}\tilde{Y}-2\tilde{x}\partial_{\tilde{x}}\tilde{Y}\ . \tag{D29}$$

d. Final scaling form

Combining Eqs. (D22), (D23) and (D28) we can express our result in terms of a universal scaling function $\mathcal{Z}_{\tilde{w}}$ as (we scale $y=\tilde{y}/m$, $\lambda_i=\frac{m^3}{\sigma}\tilde{\lambda}_i$, $W=\tilde{w}/W_\mu$):

$$\begin{aligned}&\hat{Z}^{c;\phi_1,\phi_2}_{\tilde{w}/W_\mu}\left(\frac{m^3}{\sigma}\tilde{\lambda}_1,\frac{m^3}{\sigma}\tilde{\lambda}_2\right)\\&\quad=\ \frac{1}{(Lm)^{d-1}}\frac{1}{(mS_m)^2}\times\hat{\mathcal{Z}}_{\tilde{w}}(\tilde{\lambda}_1,\tilde{\lambda}_2,\tilde{y})\end{aligned} \tag{D30}$$

The quantities W_μ and S_m are as in Eq. (90) with here $\mu=m$ (SR elasticity) and

$$\begin{aligned}\mathcal{Z}_{\tilde{w}}(\tilde{\lambda}_1,\tilde{\lambda}_2,\tilde{y})=A_d\Delta^{*\prime\prime}(\tilde{w})\times\\ \int_{\tilde{x}}\tilde{\chi}(\tilde{\lambda}_1,\tilde{x})\tilde{Y}(\tilde{\lambda}_1,\tilde{x})\tilde{Y}(\tilde{\lambda}_2,\tilde{x}-\tilde{y})\tilde{\chi}(\tilde{\lambda}_2,\tilde{x}-\tilde{y})\ ,\end{aligned} \tag{D31}$$

where $\tilde{Y}$ and $\tilde{\chi}$ are explicit functions given in Eqs. (D25) and (D29). This is our final result; its explicit evaluation is left for the future.

Appendix E: First moment to one-loop order

In this appendix we give the result for $\langle S_1^2S_2\rangle_{\rho^c_W}$ to one-loop accuracy for short-ranged elasticity. Note that since the formula (40) is exact, it does not receive higher-loop contributions and the first improvement brought to moments of ρ^c_W is for $\langle S_1^2S_2\rangle_{\rho^c_W}$. The latter can be obtained from the known formulas (61) and (118) of Ref. [31],

$$\begin{aligned}\hat{C}^{(3)}(w_1,w_2,w_3)=-\frac{6}{m^2}\mathrm{sym}_{123}\Big\{\Delta'(w_{12})\Delta(w_{13})\Big\}\\ -6I_3\,\mathrm{sym}_{123}\Big\{\Delta'(w_{12})^2\Delta'(w_{13})+[\Delta(w_{12})-\Delta(0)]\\ \times\left[\Delta'(w_{13})\Delta''(w_{12})+\Delta'(w_{12})\Delta''(w_{13})\right.\\ \left.+\Delta'(w_{23})\Delta''(w_{13})\right]\Big\}\ .\end{aligned} \tag{E1}$$

The first line corresponds to the improved tree approximation, sym_{123} denotes the symmetrization over the w_i variables, $I_3=\int_k\frac{1}{(k^2+m^2)^3}$, and we have use the shorthand notation $w_{ij}:=w_i-w_j$. As explained in the text, this formula is sufficient to obtain $\langle S_1^2S_2\rangle_{\rho^c_W}$ using the $\mathcal{K}$ operation. The final result reads

$$\begin{aligned}L^{-2d}\langle S_1^2S_2\rangle_{\rho^c_W}=-6S_m\\ -4I_3\frac{S_m}{L^dm^2}\Big[\Delta''(0)\Delta''(W)+3\Delta''(W)^2\\ +3\Delta'(W)\Delta'''(W)\Big]+O(\epsilon^3)\ .\end{aligned} \tag{E2}$$

[1] D. Fisher, "Collective transport in random media: From superconductors to earthquakes," *Phys. Rep.*, vol. 301, pp. 113–150, 1998.

[2] G. Blatter, M. Feigel'man, V. Geshkenbein, A. Larkin, and V. Vinokur, "Vortices in high-temperature superconductors," *Rev. Mod. Phys.*, vol. 66, p. 1125, 1994.

[3] T. Nattermann and S. Scheidl, "Vortex-glass phases in type-II superconductors," *Advances in Physics*, vol. 49, pp. 607–704, 2000.

[4] T. Giamarchi and P. Le Doussal, "Statics and dynamics of disordered elastic systems," in *Spin glasses and random fields* (A. Young, ed.), Singapore: World Scientific, 1997.

[5] S. Zapperi, P. Cizeau, G. Durin, and H. E. Stanley, "Dynamics of a ferromagnetic domain wall: Avalanches, depinning transition, and the Barkhausen effect," *Phys. Rev. B*, vol. 58, pp. 6353–6366, 1998.

[6] G. Durin and S. Zapperi, "Scaling exponents for Barkhausen avalanches in polycrystalline and amorphous ferromagnets," *Phys. Rev. Lett.*, vol. 84, pp. 4705–4708, May 2000.

[7] S. Moulinet, C. Guthmann, and E. Rolley, "Roughness and dynamics of a contact line of a viscous fluid on a disordered substrate," *Eur. Phys. J. E*, vol. 8, pp. 437–443, 2002.

[8] P. Le Doussal, K. Wiese, S. Moulinet, and E. Rolley, "Height fluctuations of a contact line: A direct measurement of the renormalized disorder correlator," *EPL*, vol. 87, p. 56001, 2009.

[9] Y. Ben-Zion and J. Rice, "Earthquake failure sequences along a cellular fault zone in a three-dimensional elastic solid containing asperity and nonasperity regions," *Journal of Geophysical Research*, vol. 98, no. B8, pp. 14109–14131, 1993.

[10] D. S. Fisher, K. Dahmen, S. Ramanathan, and Y. Ben-Zion, "Statistics of earthquakes in simple models of heterogeneous faults," *Phys. Rev. Lett.*, vol. 78, pp. 4885–4888, Jun 1997.

[11] L. Ponson, "Depinning transition in failure of inhomogeneous brittle materials," *Phys. Rev. Lett.*, vol. 103, p. 055501, 2009.

[12] S. Santucci, M. Grob, R. Toussaint, J. Schmittbuhl, A. Hansen, and K. J. Maly, "Fracture roughness scaling: A case study on planar cracks," *EPL (Europhysics Letters)*, vol. 92, no. 4, p. 44001, 2010.

[13] D. Bonamy, S. Santucci, and L. Ponson, "Crackling dynamics in material failure as the signature of a self-organized dynamic phase transition," *Phys. Rev. Lett.*, vol. 101, no. 4, p. 045501, 2008.

[14] R. Planet, S. Santucci, and J. Ortín, "Avalanches and non-gaussian fluctuations of the global velocity of imbibition fronts," *Phys. Rev. Lett.*, vol. 102, p. 094502, Mar

2009.
[15] J. Sethna, K. Dahmen, and C. Myers, "Crackling noise," *Nature*, vol. 410, pp. 242–250, 2001.
[16] L. E. Aragn, A. B. Kolton, P. L. Doussal, K. J. Wiese, and E. A. Jagla, "Avalanches in tip-driven interfaces in random media," *EPL (Europhysics Letters)*, vol. 113, no. 1, p. 10002, 2016.
[17] G. Durin, F. Bohn, M. A. Correa, R. L. Sommer, P. Le Doussal, and K. J. Wiese, "Quantitative scaling of magnetic avalanches," *ArXiv e-prints*, Jan. 2016.
[18] F. Omori, "On the aftershocks of earthquakes," *Journal of the College of Science, Imperial University of Tokyo*, vol. 7, pp. 111–200.
[19] R. Burridge and L. Knopoff, "Model and theoretical seismicity," *Bulletin of the Seismological Society of America*, vol. 57, no. 3, pp. 341–371, 1967.
[20] E. Jagla and A. Kolton, "The mechanisms of spatial and temporal earthquake clustering," *arXiv:*, vol. 0901.1907, 2009.
[21] E. A. Jagla, F. P. Landes, and A. Rosso, "Viscoelastic effects in avalanche dynamics: A key to earthquake statistics," *Phys. Rev. Lett.*, vol. 112, p. 174301, Apr 2014.
[22] E. A. Jagla, "Aftershock production rate of driven viscoelastic interfaces," *Phys. Rev. E*, vol. 90, p. 042129, Oct 2014.
[23] A. Dobrinevski, P. Le Doussal, and K. J. Wiese, "Statistics of avalanches with relaxation and barkhausen noise: A solvable model," *Phys. Rev. E*, vol. 88, p. 032106, Sep 2013.
[24] D. S. Fisher, "Interface fluctuations in disordered systems: $5-\epsilon$ expansion and failure of dimensional reduction," *Phys. Rev. Lett.*, vol. 56, May 1986.
[25] T. Nattermann, S. Stepanow, L.-H. Tang, and H. Leschhorn, "Dynamics of interface depinning in a disordered medium," *J. Phys. II (France)*, vol. 2, pp. 1483–8, 1992.
[26] O. Narayan and D. S. Fisher, "Critical behavior of sliding charge-density waves in 4-epsilon dimensions," *Phys. Rev. B*, vol. 46, pp. 11520–49, 1992.
[27] O. Narayan and D. S. Fisher, "Threshold critical dynamics of driven interfaces in random media," *Phys. Rev. B*, vol. 48, pp. 7030–42, 1993.
[28] P. Chauve, P. Le Doussal, and K. Wiese, "Renormalization of pinned elastic systems: How does it work beyond one loop?," *Phys. Rev. Lett.*, vol. 86, pp. 1785–1788, 2001.
[29] P. Le Doussal, K. J. Wiese, and P. Chauve, "2-loop functional renormalization group analysis of the depinning transition," *Phys. Rev. B*, vol. 66, p. 174201, 2002.
[30] P. Le Doussal, K. J. Wiese, and P. Chauve, "Functional renormalization group and the field theory of disordered elastic systems," *Phys. Rev. E*, vol. 69, p. 026112, 2004.
[31] P. Le Doussal and K. J. Wiese, "Size distributions of shocks and static avalanches from the functional renormalization group," *Phys. Rev. E*, vol. 79, p. 051106, 2009.
[32] P. Le Doussal and K. J. Wiese, "First-principle derivation of static avalanche-size distribution," *Phys. Rev. E*, vol. 85, p. 061102, 2012.
[33] P. Le Doussal and K. J. Wiese, "Avalanche dynamics of elastic interfaces," *Phys. Rev. E*, vol. 88, p. 022106, Aug 2013.
[34] M. Delorme, P. Le Doussal, and K. Wiese, "Distribution of joint local and total size and of extension for avalanches in the Brownian force model," *ArXiv e-prints*, Jan. 2016.
[35] T. Thiery, P. Le Doussal, and K. J. Wiese, "Spatial shape of avalanches in the brownian force model," *Journal of Statistical Mechanics: Theory and Experiment*, vol. 2015, no. 8, p. P08019, 2015.
[36] A. Dobrinevski, P. Le Doussal, and K. Wiese, "Avalanche shape and exponents beyond mean-field theory," *EPL*, vol. 108, p. 66002, 2014.
[37] B. Alessandro, C. Beatrice, G. Bertotti, and A. Montorsi, "Domain-wall dynamics and Barkhausen effect in metallic ferromagnetic materials. I. Theory," *J. Appl. Phys.*, vol. 68, p. 2901, 1990.
[38] B. Alessandro, C. Beatrice, G. Bertotti, and A. Montorsi, "Domain-wall dynamics and Barkhausen effect in metallic ferromagnetic materials. II. Experiments," *Journal of Applied Physics*, vol. 68, no. 6, p. 2908, 1990.
[39] P. Le Doussal, "Finite temperature Functional RG, droplets and decaying Burgers turbulence," *Europhys. Lett.*, vol. 76, pp. 457–463, 2006.
[40] A. A. Middleton, P. Le Doussal, and K. J. Wiese, "Measuring functional renormalization group fixed-point functions for pinned manifolds," *Phys. Rev. Lett.*, vol. 98, p. 155701, 2007.
[41] P. Le Doussal, "Exact results and open questions in first principle functional RG," *Annals of Physics*, vol. 325, pp. 49–150, 2009.
[42] L. Carraro and J. Duchon, "Équation de Burgers avec conditions initiales à accroissements indépendants et homogènes," *Ann. Inst. Henri Poincaré*, vol. 15, pp. 431–458, 1998.
[43] P. Le Doussal and K. J. Wiese, "Driven particle in a random landscape: disorder correlator, avalanche distribution and extreme value statistics of records," *Phys. Rev. E*, vol. 79, p. 051105, 2009.

Contents

I. Introduction 1

II. Main results 2

III. Model, shock observables and method 4
A. Model 4
B. The ground state and the scaling limit 4
C. Properties of $\tilde{\Delta}^*(u)$ and static universality classes 5
D. Shocks observables: Densities 5
E. Shocks observables: Probabilities 6
F. Relation between avalanche-size moments and renormalized force cumulants: First moment 6
G. Generating functions 7
H. Relation between avalanche-size moments and renormalized force cumulants: Kolmogorov cumulants and chain rule 7
I. Strategy of the calculation and validity of the results 8
J. Connected versus non-connected averages and the ϵ-expansion 8

IV. Correlations between total shock sizes 9

A. Reminder of the diagrammatic rules and extraction of shock moments 9
B. Lowest moments 9
C. Generating function for all moments 10
D. Results for the densities 10
E. Analysis of the results 11

V. Local structure of correlations 12
A. Reminder: one-shock case 12
B. Two-shock case: Notation and diagrammatic result 13
C. First moments: arbitrary sources and kernels 14
D. First moment: correlations between the local shock sizes for short-ranged elasticity. 14
E. First moment: correlations between the local shock sizes for long-ranged elasticity. 15

VI. Measurement of correlations in simulations of $d = 0$ toy models. 15
A. Models and goals 15
B. Numerical Results: RB model 16
C. Numerical Results: RF model 16

VII. Conclusion 17

Acknowledgments 18

A. Proof of the identity on generating functions 18

B. Diagrammatic rules for two-shocks moments 18

C. A derivation from the Carraro-Duchon formula 19

D. Saddle-point calculation for the local structure. 20
1. Algebraic derivation of Eq. (107) 20
a. Solutions for the u variables 21
b. Solutions for the U variables 21
c. Final result 22
d. Simplified form of the final result 22
2. More explicit solution for avalanches measured on parallel hyperplanes 22
a. Setting 22
b. Solution for Y 22
c. Solution for χ 22
d. Final scaling form 23

E. First moment to one-loop order 23

References 23